Journal of Solid State Electrochemistry (2019) 23:1947–1965
https://doi.org/10.1007/s10008-019-04291-9

REVIEW

About the capacitive currents in conducting polymers: the case of polyaniline

Juliana Scotto[1,2] · Waldemar A. Marmisollé[1] · Dionisio Posadas[1]

Received: 28 March 2019 / Revised: 29 April 2019 / Accepted: 30 April 2019 / Published online: 11 June 2019

Abstract

In the present work, we review the occurrence of capacitive currents in conducting polymer and, particularly, in the electrochemical response of polyaniline film-coated electrodes Firstly, we present and discuss the differences between the electrical double-layer capacitance and the so-called pseudocapacitance. Then, we discuss the capacitive behavior of Pani as studied by a variety of electrochemical (cyclic voltammetry, electrochemical impedance spectroscopy) and spectroscopic techniques (*epr*, UV-visible). Understanding the capacitive behavior of polyaniline (Pani) becomes essential not only from an academic point-of-view but also from a technological perspective, as Pani has been extensively employed for the construction of materials for supercapacitors.

Keywords Capacitance · Pseudocapacitance · Double layer · Constant phase element · Cyclic voltammetry · Polyaniline

Introduction

In the last years, there has been an increasing interest in the development of batteries, mainly those related to Li, and also in the so-called supercapacitors [1]. This has motivated to scientists working in material science to move their interest into this field. Obviously, the fundamental aspects of these devices are electrochemical and sometimes, it seems that possibly not everybody is aware of the subtleties of some electrochemical concepts related to them. This fact usually generates some confusion about the true nature of the processes that may arise in such devices. The entrance of material science to the electrochemical field has undoubtedly prompted its frontiers and brought an impelling fresh air to this area.

Pani has been one of the most employed materials for the construction of supercapacitors with different architectures [2], such as supercapacitors based on highly porous Pani [3], Pani nanofibers [4–7], self-doped nanofibers [8], nanowires [9, 10], and other nanostructures [11, 12]. Additionally, the combination of Pani with other materials seems to be a very promising field [13]. Recently, plenty of works report the performances of Pani composites with different types of materials such as, carbon nanostructures [14–16], carbon nanotubes [17], graphene [18–21], few-layer graphene [22], graphene oxide [23, 24], reduced graphene oxide [25], and even inorganic materials, such as silica [26], ITO [27], and MnO_2 [28].

Within this framework, the purpose of this work is to review the supposedly double-layer capacitive response of conducting polymers, in particular of polyaniline (Pani). Furthermore, since this double-layer capacitance may occur together with, or may even be a consequence of, the occurrence of a pseudocapacitive current, we will first refer to the differences of these two types of responses.

Dedicated to the memory of Dr. María Inés Florit who recently passed away.

✉ Dionisio Posadas
dposadas@inifta.unlp.edu.ar

[1] Instituto de Investigaciones Fisicoquímicas Teóricas y Aplicadas (INIFTA). Facultad de Ciencias Exactas, Universidad Nacional de La Plata, CCT La Plata-CONICET, Suc. 4, CC 16, 1900 La Plata, Argentina

[2] Instituto de Ciencias de la Salud, Universidad Nacional Arturo Jauretche, Av. Calchaquí 6200, Florencio Varela, Buenos Aires, Argentina

Electrochemical double-layer capacitance and pseudocapacitance

The electrochemical double-layer capacitance

We will consider only flat surfaces in opposition to rough surfaces. According to de Levie [29], it is possible to distinguish three types of roughness (r); geometric roughness, with dimensions in the order of millimeters; atomic roughness, in

the order of nanometers and smaller; and intermediate roughness; in between the two mentioned above, in the range between 10 to 0.1 mm. In this work, we will be concerned with the last two cases. Atomic scale defects comprise kinks, steps, screws, and voids at the solid surface. It deserves to point out that, in polycrystalline materials, different crystallographic planes have different double-layer capacitances, adsorption energies, and rates of charge transfer.

Let us consider an electrode. We will say that there is *faradaic current* (j_F) flowing through an electrochemical cell when there is a net electrochemical reaction and some chemical species changes its chemical nature. The resistance for the faradaic current to flow is $R_{ct} = dE/dj_F$. On the contrary, when there are no chemical changes and the current is the result of charge movements near the interface (but not across the interface), we will say that there is a *capacitive current* (j_C).

It is important to point out that the interface we are considering is always that between the electrode material and the electrolyte solution. However, the electrode material may be quite different in nature: a metal, a semiconductor, another non-miscible solution, a polymer capable of conducting current or transport charged particles, and so on. If at each side of the interface, there is charge accumulation, *an electrochemical capacitor* is formed. At the solution side of the electrode/solution interface, there is a charge distribution that may be considered as composed of two regions: a compact layer, of capacitance C_H, and a diffuse region of capacitance C_d. As a consequence, this model of the charge reorganization within the electrolyte solution due to the presence of a charged phase is often called double layer [30]. The total double-layer capacitance C_{dl} is equal to $C_{dl} = C_d C_H/(C_d + C_H)$. At electrolyte concentrations above 10^{-2} M, in the absence of ionic specific adsorption, C_{dl} is practically independent of the concentration. This notion of the interface is based on the Stern- Grahame-Gouy-Chapman model to describe the solution side of the double layer [30]. However, we will pay no attention to double layers at the electrode material side [31], nor to double layers at the interfaces film/solution as occurs in many film electrodes.

For the time being, we will consider the interface to be a metal in contact with an electrolytic solution as represented, in electrical terms, in Scheme 1. Here, R_{ct} is the charge transfer resistance at the metal surface of the occurring electrochemical reaction, and R_s is the solution resistance between an external point of the electrical double layer and the tip of the Luggin capillary. For future reference, in Fig. 1, it is schematically represented the CV and the electrochemical impedance spectroscopy (EIS) responses of the circuit represented in Scheme 1. Values of the relevant parameters are specified in the captions. Note that, in the calculation of the voltammetric response, C_{dl} is assumed to be independent of the applied potential, E. This is not the case for most metals (see, for instance, [32–34]). The behavior of the capacitance depicted in this figure is often called *ideal capacitance*.

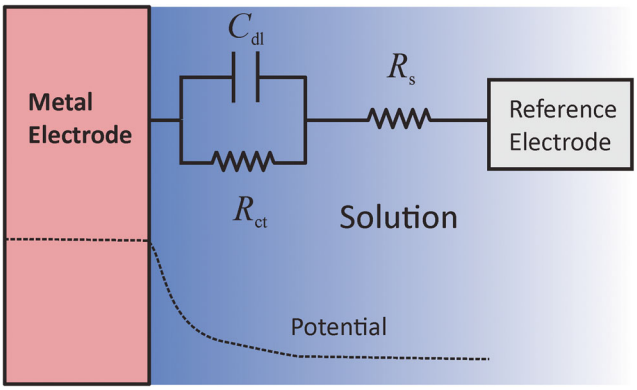

Scheme 1 Electrical representation of an interface metal/solution

Blocking electrodes and electrochemical double-layer capacitance

If it is not possible the charge transfer at the metal/electrolyte solution interface ($R_{ct} \approx \infty$, red lines in Fig. 1), a purely capacitive current will flow, due to the fact that the interface becomes more or less charged as the potential difference is changed. This is an *ideally polarizable interface* (IPI). Actually, if an electrochemical reaction is going on in the potential region of limiting diffusion regime, the interface may also be an IPI [32]. This kind of interface is often called a *blocking electrode*. A real system that quite closely approaches to this situation is a mercury electrode in KCl solution, in the potential range from 0.3 to 1.8 V (vs. SCE) [32].

Red lines in Fig. 1 correspond to the behavior expected for this kind of interfaces. Particularly when considering cyclic voltammetry, there are some features that can be associated to a purely capacitive response: (i) the current is linearly dependent on the sweep rate, v; (ii) the current is constant (C_{dl} independent of E) in a wide range of potentials (except near the limits of the potential scan); and (iii) if the potential scan is stopped ($v = 0$), the current would go to zero. Moreover, the slope of a representation of the current as a function of the sweep rate directly gives the capacitance of the electrode (usually referred to as differential capacitance, C_d).

The influence of the charge transfer resistance

On the other side, if there is some substance in solution, or even the electrode, capable of become reduced or oxidized, there will be, added in parallel to the charging capacitive current, a faradaic current flow due to the redox process. Note that if the two components of the redox couple were present, and the couple had an extremely high exchange current (R_{ct} very small); then, at equilibrium, the potential would be fixed at the value corresponding to that of the formal potential of the redox couple. This constitutes what it is called a *non-polarizable interface* (NPI). The thermodynamic of both interfaces have been extensively studied [35, 36]. In general, both

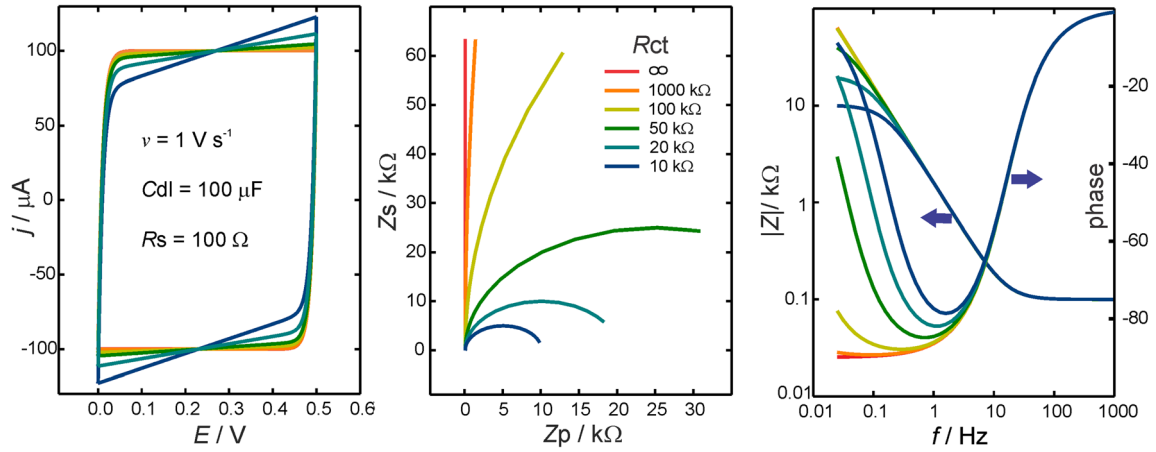

Fig. 1 Calculated representation of the CV (**a**), $v = 1\ \mathrm{V\ s^{-1}}$ and EIS responses of the circuit in Scheme 1, in the form of Nyquist (**b**) and Bode (**c**) plots for $R_s = 100\ \Omega$, $C_{dl} = 100\ \mu\mathrm{F}$, and different values of R_{ct} (given in the plots)

components of the redox couple could be adsorbed at the interface; then, as it is not possible to distinguish which fraction of the current goes to charge the double layer and which one to change the surface concentrations of the redox couple, the thermodynamic charge is undetermined. Under these conditions, the charge (in the Lippmann's sense, that is, the excess or defect of charge, due to free carriers at each side of the interface) is not defined [35, 36]. That is, the thermodynamic charge cannot be measured. This fact makes the double-layer capacitance to be also undefined.

In general, it is not possible, unless some extra assumptions are considered, to separate the capacitive from the faradaic charge. Often, under the assumption that the capacitive current is very small and independent of the faradaic process, a base line is drawn and discounted from the total current, that is the sum of the capacitive and the faradaic currents. However, this procedure may lead to serious errors, as it is the case of conducting polymers (see below).

The effect of the R_{ct} on the voltammetric and the EIS responses is also illustrated in Fig. 1. In the CV response, the presence of a finite R_{ct} distorts the capacitive plateau inducing a slope, whereas in the Nyquist plot, the straight vertical response shifts the phase to lower values, drawing a semi-circle. The lower the values of the charge transfer resistance, the more noticeable this effect is.

The relative influence of the charge transfer resistance on the voltammetric response is also higher for low scan rates, as depicted in Fig. 2. In this figure, the simulated voltammetric response was computed by considering a defined constant value for R_{ct} in the whole potential range, which could not be the most general case. However, the analysis of this figure allows concluding that even for a constant R_{ct}, the voltammograms are no longer that of a purely capacitive response: the capacitive plateau disappears and current is not strictly linear on the sweep rate. Nevertheless, the width of the voltammograms is still constant and a plot of $(j_{an} - j_{cat})/2$ against the sweep rate allows obtaining the differential capacitance [37], which still coincides with the true C_{dl} of the equivalent circuit in Scheme 1.

The true values of the C_{dl} can be also obtained more directly by non-linear fitting of the EIS response to the complete equivalent circuit.

Pseudocapacitance

Electroactive adsorbed species

Let us consider now an electrochemical reaction like the formation of atomic hydrogen on an electrode [38]:

$$H_3O^+ + M + e_M \underset{V_b}{\overset{V_d}{\leftrightarrow}} H_{ad}\cdots M + H_2O \qquad (1)$$

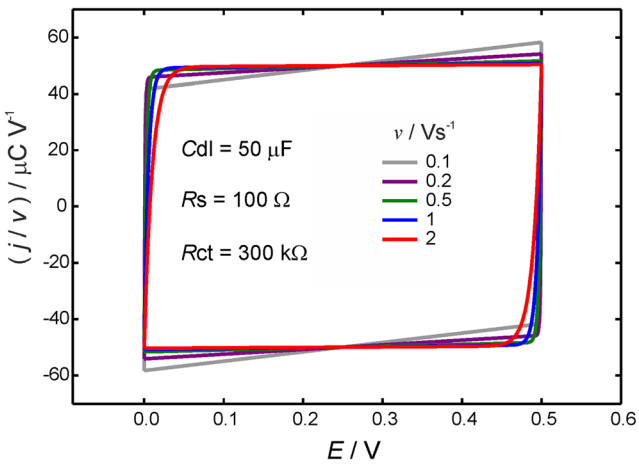

Fig. 2 Effect of the sweep rate on the distortion of the purely capacitive voltammetric response by the polarization resistance. Note that the function plotted is the current divided by the sweep rate. Values of the parameters are presented in the plot

where M is a metal atom at the metallic side of the interface, e_M is an electron at the metal, $H_{ad}\cdots M$ is an adsorbed hydrogen atom on the surface, and v_d and v_b are the direct and backward rates. Reaction (1) is an example of what Conway [1] call a two-dimensional electrosorption, also known as *underpotential deposition* (UPD).

When v_d and v_b are sufficiently high, reaction (1) can be considered at equilibrium at each potential and the reaction is called *reversible*. For an infinitesimal change in the potential, dE, an infinitesimal change in the surface concentration of adatoms will occur, $d\Gamma_H$, giving rise to an infinitesimal flow of faradaic charge, $dq = F\, d\Gamma_H$, so that a capacitance can be defined as:

$$C_f = dq/dE$$

If the only electrochemical process that occurs is that represented by Eq. (1), then, after a potential step, the current transient would go to zero. Moreover, the voltammetric current at any potential does linearly depend on the sweep rate as it happens for capacitive processes. The formal similarities between this process and the charging of an electrical capacitor lead to the name of *pseudocapacitance* for C_f. The subscript *f* emphasizes the idea of a faradaic process.

However, it is clear that its nature differs completely from that of the charging of a capacitor. Moreover, there is an important difference between the double-layer capacitance and a pseudocapacitance like that due to reaction (1). The transfer of charge occurs on a substance very near to or adsorbed on the electrode surface and there is no diffusional control at the solution side. Therefore, the charge is proportional to the *real surface area*.

For the sake of future reference, the current-potential relationship for this process is represented in Fig. 3. In some cases it is necessary to consider interactions between the adsorbed atoms or some other type of surface heterogeneity (see, for instance, [38, 40]). This is also called non ideal reversible charge transfer. The CV response in the presence of interactions is also shown in Fig. 3. Note that in a real process, if the H_3O^+ concentration is too low or if the sweep rate too high the CV response would no longer that shown in Fig. 3 and the peak current will depend on $v^{1/2}$.

The equations for the current response of pseudocapacitive processes like that of Eq. (1) during a linear potential sweep have been worked out by Gileadi and Srinivasan [41]. These authors considered adsorbed species under both reversible and irreversible charge transfer controls (see below).

The characteristic electrochemical parameters in CV are the peak potential and current. For a reversible reaction as that represented in reaction (1), they have the following characteristics: (i) both the anodic and the cathodic current peaks are equal and depend linearly on the scan rate; (ii) both the anodic and cathodic peaks potentials are equal and independent of v; (iii) the current depends linearly on the surface concentration (in this case, the voltammetric total charge).

In the case of a totally irreversible reaction, only v_d needs to be considered [30, 41] and the characteristic electrochemical parameters (potential and peak current) depend on the sweep rate. However, the current is still linearly increasing on the sweep rate (Fig. 4). It can be seen that in the presence of interactions, the influence of the interaction parameter is similar to that of the reversible case (Fig. 4).

It is interesting to discuss how is the EIS response for a process like that described in Eq. (1) and in Fig. 3 (electrochemically reversible process). In this case, it is clear that R_{ct} is in series with the pseudocapacitance, because the charge develops by the occurrence of the electrochemical reaction. Therefore, the Nyquist plot should give a vertical straight line like that shown in Fig. 1 for $R_{ct} = \infty$ (blocking electrode). However, here, R_{ct} is not infinite but rather, on the contrary, it is very small ($R_{ct} \to 0$). The case of an irreversible

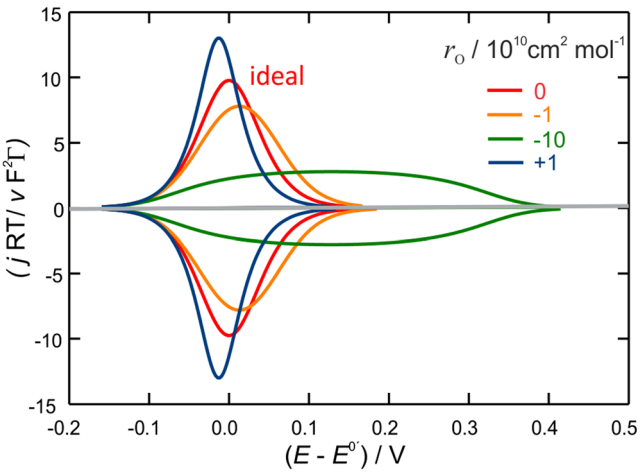

Fig. 3 Dimensionless current density vs. potential for an electrochemically reversible process. Values of the interaction parameters in the plot. $r_R = 0$ cm^2 mol^{-1}, $n = 1$, $E^{0'} = 0$ V. See [39]

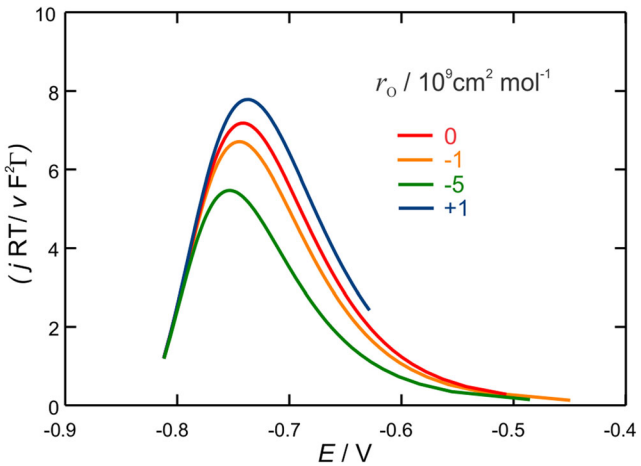

Fig. 4 Simulated dimensionless current density vs. potential for an electrochemically irreversible process. $\Gamma^*_{ox} = 2 \times 10^{-10}$ mol cm^{-2}, $k_0 = 1 \times 10^{-9}$ s^{-1}, $r_R = 0$ cm^2 mol^{-1}, $n = 1$, $E^{0'} = 0$ V. The calculations are based on the approximation of considering only the two first terms in the expansion of the exponential function [41]

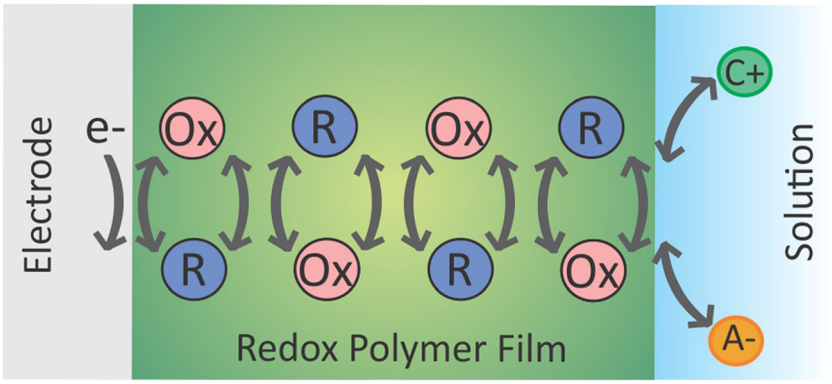

Scheme 2 Electrode covered by a redox polymer film. R and Ox are the components of the redox couple. A^- and C^+ are anions and cations, present in the internal and the external solutions. Note that in the absence of a redox couple in the external solution, there is an *ionic charge transfer* at the polymer/solution interface

electrochemical reaction is similar (R_{ct} is not small). However, in a real situation, reaction (1) will still be in parallel with C_{dl}.

Note that, so far, one of the conditions for a pseudocapacitance to appear is that one or both of the species participants in the reaction are at the interface (in this case, adsorbed). This would not happen if the two components of the redox couple are in solution (e.g., Fe^{3+}/Fe^{2+}). The other condition is the existence of charge transfer, which implies the chemical transformation of some species. In line with the previously discussed ideas, it can be said that the origin of the pseudocapacitance is not a capacitive but a faradaic process. There are many other types of processes in which a pseudocapacitance appears. Let us mention confined redox couples and film-covered electrodes. In the latter case, there are electrochemically active polymers (EAPs). EAPs are polymers that can be oxidized and reduced reversibly (see Scheme 2). They are divided in redox polymers (RPs), which are not intrinsically conducting, and conducting polymers (CPs). For thin polymer films, the electrochemical response of redox polymers very often is exactly as that depicted in Fig. 3.

The voltammetric response of Pani

It is well known that the voltammetric response of CP shows, after the first current peak, and in the potential region where the polymer becomes electronically conductor, a current plateau that present the characteristics of a capacitive current [42–44] (see Fig. 5). As an example, we show the CV of Pani in acid media in Fig. 5. There has been a controversy about the nature of this capacitance among the workers in the field. On one side, it is believed that is pseudocapacitive in origin; that is, it is a consequence of a surface redox reaction much in the same way that it happens at the surface of RuO_2 [1]. That is, it is a consequence of a faradaic redox reaction. On the other hand, it is thought that it is of the usual double-layer capacitance due to charge separation at the interface.

Although this capacitive behavior is present in all conductive polymers, because in Pani it has been much more studied, we will concentrate almost exclusively on this polymer. Because the electrochemistry of Pani has been intensively and extensively studied applying a wide variety of in situ and ex situ techniques, we will refer to those investigations directly related to the capacitive currents.

Before discussing the capacitive currents, we will give a brief qualitative description of the processes involved during the oxidation of leucoemeraldine to emeraldine and vice versa.

It is widely recognized that in the case of Pani [46, 47], the reduced centers are the amino groups and the oxidized ones are amino groups (see Scheme 3).

As demonstrated by Peter et al. [48], both the oxidation/reduction processes of Pani are very fast. On the other hand, the CV response can be represented by a kinetics corresponding to an electrochemical reversible process with interactions between the redox centers [45]. These interactions are electrostatic in nature and come from the protonated amino and amino groups. Therefore, they depend on the pH of the external solution [49, 50]. The dissociation constants, K_a, of both leucoemeraldine (LE) and emeraldine (E) are measured

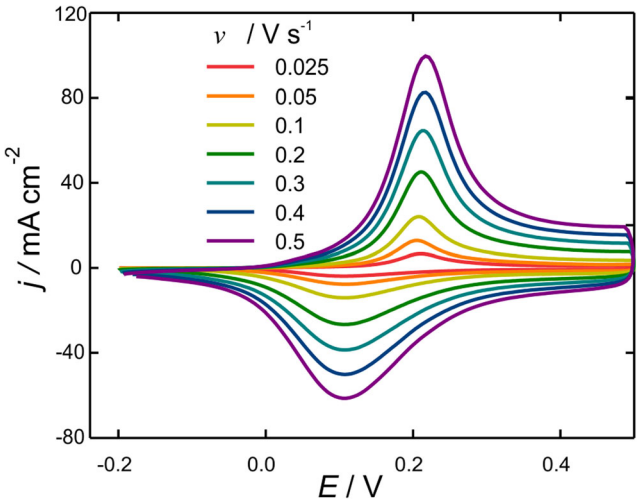

Fig. 5 Voltammetric response of Pani during its half oxidation in 3.7 M H_2SO_4. Voltammetric charge, $Q_T = 34$ mC cm^{-2}. Potentials are referred to SCE. Note the capacitive current after the current peak [45]

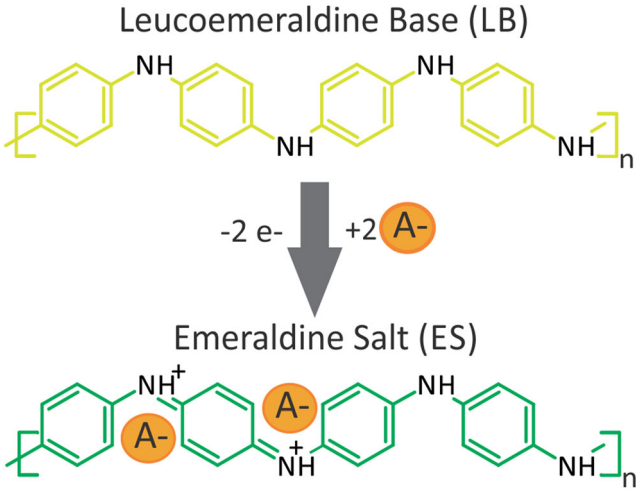

Scheme 3 Scheme showing the reduced form of leucoemeraldine base (top) and the half oxidized form of the emeraldine salt (bottom). Here, A means the counterions needed for charge neutralization

several times (see [51] and references therein). $K_{a,LE}$ is about 0.5 and $K_{a,E}$ is about 4.5. This means that in the pH range where PANI is electroactive ($-1.0 < pH < 4.5$), the E form will be almost fully protonated but at $pH > 1.0$, the LE form will be deprotonated. Incidentally, it is good to emphasize at this point that the presence of interactions affects the formal potential so as to produce a distribution of formal potentials.

There are several processes going on when considering the redox behavior of Pani, even at equilibrium, in the system: bare metal plus a polymer film on top of the metal contacting the solution side at the other end. There is an electronic charge transfer at the metal/polymer interface according to Scheme 3; there is charge transport across the film by a mixed electron/ion mechanism (see, for instance [52]) and ionic charge transfer at the polymer/solution interface. It is interesting to point out that during current flow, in the absence of redox couples in the external solution, only ionic charge transfer occurs at the polymer/solution interface. In the presence of redox couples, in a transient experiment, there will also be electronic current due to the occurrence of an electrochemical reaction at the polymer/solution interface. Under a steady-state polarization condition, there will be, after the steady state is reached, only electronic current. In the case of conducting polymers, it is interesting to note that the electrochemical reaction of the redox couple proceeds as if it were on a metal.

Also, there is a proton binding process at the polymer fibrils in contact with the internal solution. As a consequence of the proton binding, counter ions ingress the film to screen the proton charges (counter ions could conceivable bind specifically the proton centers or they even may form ionic pairs). As a consequence of charge transfer, one species transforms into another and there are also changes of volume of the polymer. Such changes have been measured experimentally [53]. As a consequence of those volume changes, the mechanical state of the polymer changes. These volume changes are then accompanied by ion ingress/egress and swelling/deswelling of the polymer.

The latter changes have been observed many times by different techniques such as radiotracers [54, 55], EQMB [56–61], ex situ infrared spectroscopy [62], scanning electrochemical microscopy [63], probe beam deflection [64], UV-visible spectroscopy [65, 66], ring-disk rotating electrode [67], and combined EQCM and surface plasmon resonance [68].

The Donnan potential at the polymer/external solution interface depends on the amount of protonated sites (fixed sites) within the polymer ant the total ionic strength in the external solution.

Both the nature of the accompanying anion and the ionic strength of the external solution affect the electrochemical response and other properties of Pani through several and different effects. Thus, on one side, as the ionic strength of the external electrolyte decreases the absolute value of the Donnan potential established at the polymer/external solution interface increase [69]. Also, the stability of the polymers towards potential cycling at different pHs depends on the nature of the accompanying anion [70]. For instance, as the pH increases, the stability limit decreases in the order $HCl > HClO_4 > H_2SO_4$. On the other hand, the acidity constant of LE form depends on the nature of the anion and the ionic strength [69]. The conductivity of Pani also depends on the type of anion of the acid during the protonation of the base form of emeraldine [71–74].

The voltammetric behavior of PCs and the capacitive currents

The voltammetric response of PCs such as polypyrrole (Ppy) [42], polyaniline (Pani) [43], and polytiophene (PT) [44], starting from the most reduced state, shows a peak followed by a current plateau. On the basis of the sweep rate, v, and thickness, l, dependences of the voltammetric responses (Fig. 6), it might be inferred that the current peak is due to a pseudocapacitive process and that the current plateau is due to pure double-layer capacitance.

According to $j_{cap} = v\ C_v$, where C_v is the voltammetric capacitance, the latter can be obtained from Fig. 6.

Several voltammetric studies employing a very small voltage span (typically 10–50 mV) have been carried out [75–77] (Fig. 8). Observe the close resemblance with Figs. 1 a and 2 and note that R_{ct} should be very high.

From the sweep rate dependence of the current j_{cap} (Fig. 1), the capacitance C_v can be calculated from $C_v = j_{cap}/v$ (Fig. 6). In Fig. 7, this is shown as a function of the total integrated current up to $E = 0.45$ V, voltammetric charge, Q_T (0.45). Assuming this charge is, in same way, proportional to the total amount of material, it results that C_v is proportional to the

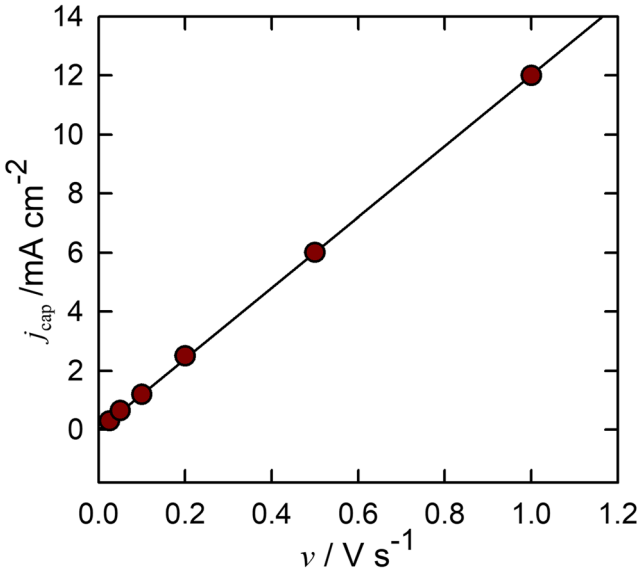

Fig. 6 Capacitive current as a function of the scan rate for a Pani film of 11 mC cm^{-2}

amount of material on the base electrode. Another fact to take into consideration is the high value of C_v of several thousands of microcoulombs per square centimeter as compared with those at the mercury/solution interface that is of a few tens of microcoulombs. Before going further, we must distinguish the interface at the polymer phase/*external* solution, which would be a geometrical area, and the interface between the polymer fibrils and the *internal* solution (see for instance [78]). Clearly, the area of this second interface will be much bigger than the first one. In view of this argument, the locus of the electrical double layer responsible of C_v must be at the polymer fibrils internal solution interface [75, 79]. Here, there has been a controversy between the supporters of the argument that the capacitance is due to a surface electrochemical reaction and those that sustain that the capacitance is due to an electrical double later. According to the formers [76, 80], in order to explain the high values of the capacitances, the fibril radius should be extremely low. According to the latter [75, 79, 81], the area of the fibril/internal solution interface should be sufficiently high to explain the high values of the observed capacitances.

Several studies of the influence of the pH of the external media on the voltammetric response have been carried out [56, 71, 82–87]. In general, it is concluded that both the current peak potential, E_p, and current, j_p, decrease with the pH in the pH range comprised between − 1 and about 2. From this value on, both E_p, and j_p increase with the pH. Beyond certain pH value (ca. 3–5), the electrochemical activity disappears. The potential range electrochemical activity depends on the nature of the accompanying anion. Most notable is the case of the chloride ions in which pHs as high as 5 may be reached. On the other hand, the capacitive current at the plateau is almost independent of the pH (Figs. 9 and 10).

Several years ago, Feldberg [81] proposed a model in which the capacitive charge, Q_C (E), is considered proportional to the faradaic one, Q_F (E) that is:

$$Q_C(E) = a\,(E - E_z)\;Q_F(E) \tag{2}$$

where a is a constant and E_z is the potential of zero charge. Taking into account the relationship $Q_T(E) = Q_C(E) + Q_F(E)$, the total current, j_T, can be obtained by differentiation with respect to the time:

$$j_T(E) = (1 + a(E - E_z))j_F + vaQ_F(E) \tag{3}$$

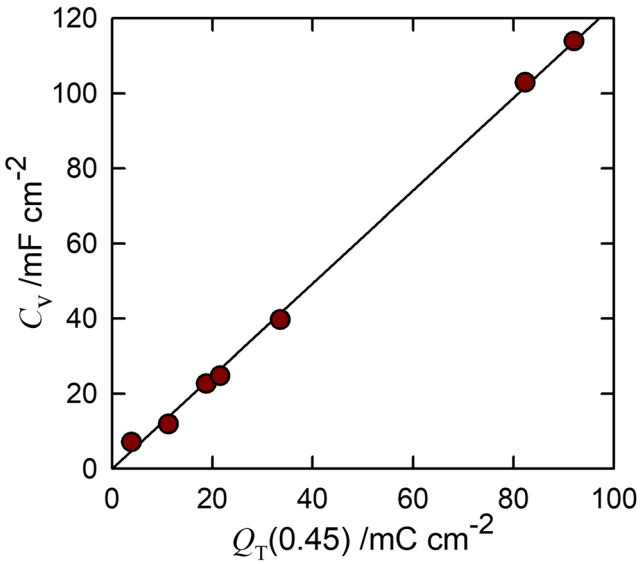

Fig. 7 Dependence of the voltammetric capacitance (C_v), on the voltammetric charge, Q_T (0.45 V). 3.7 M H_2SO_4 solution. $v = 0.1$ V s^{-1}

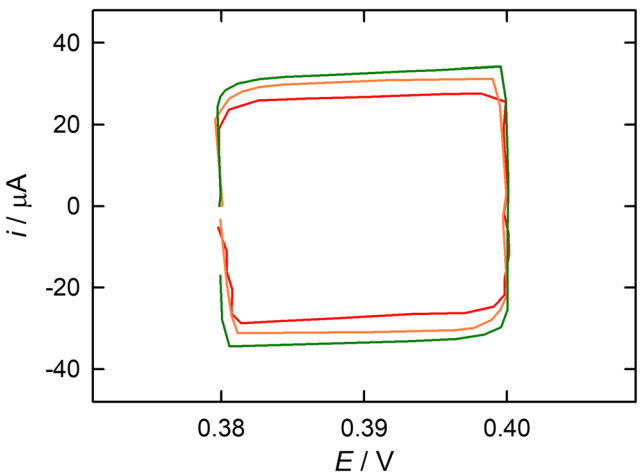

Fig. 8 Small amplitude cyclic voltammetry of Pani in the plateau region in different electrolytes. Potentials referred to the SCE. Orange: 1 M $HClO_4$ + 1 M Na ClO_4 (pH = 0.12). Green: 1 M HCl + 1 M NaCl (pH = 0.19). Red: 1 M H_2SO_4 + 1 M Na_2SO_4 (pH = 0.10). Redrawn from data of Ref. [75]

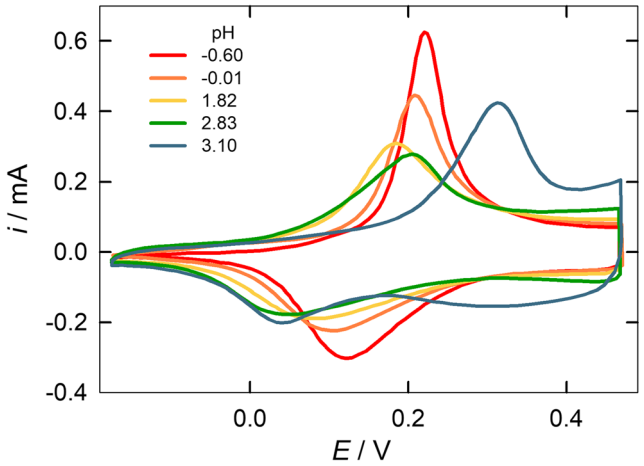

Fig. 9 Stationary cyclic voltammetry of a Pani film in $H_2SO_4 + NaHSO_4$, $\mu = 3.7$ M at different pHs. Q_T (0.45) = 20.0 mC cm^{-2}, $v = 0.01$ Vs^{-1} [50]

where $v = dE/dt$ is the sweep rate.

At high enough potentials, $E > E_L$, where the faradaic process has finished and $j_F = 0$; the current is only capacitive and:

$$Q_F(E > E_L) = Q^0 \tag{4}$$

where Q^0 is the maximum faradaic charge. From Eq. 3, it follows that:

$$j_T(E > E_L) = vaQ^0 \tag{5}$$

and

$$Q_T(E > E_L) = aQ^0\left(a^{-1} - E_z\right) + aQ^0E = \sigma C_d + C_dE \tag{6}$$

A plot of Q_T ($E > E_L$) as a function of E is shown in Fig. 11. From the slope and ordinate of this plot, it is possible to obtain C_d and σ, as defined by Eq. 6. Q^0, a, and E_z cannot be obtained

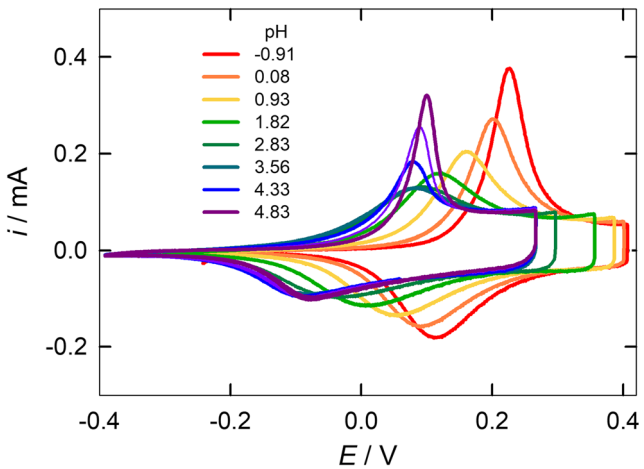

Fig. 10 Stationary cyclic voltammograms of a Pani film in HCl + NaCl, $\mu = 4$ M at different pHs. Q_T (0.45) = 24 mC cm^{-2}, $v = 0.01$ Vs^{-1} [50]

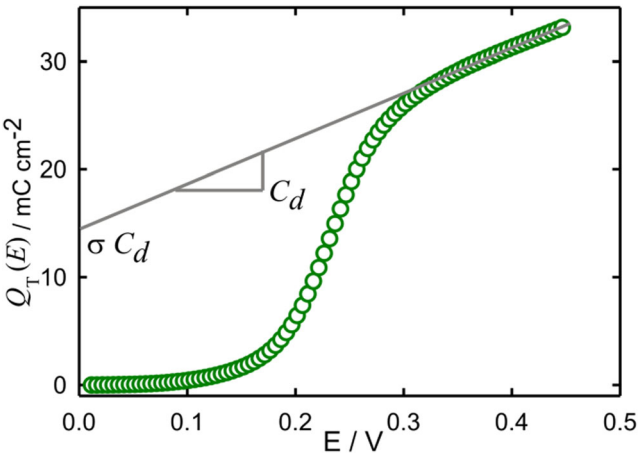

Fig. 11 Integrated voltammetric charge as a function of potential for a Pani film in 3.7 M H_2SO_4

from voltammetric experiments alone. Note that, in this case, it is not possible to separate the double-layer capacitance from the pseudocapacitance.

Taking into account the definition of the faradaic oxidation fraction, $x_{Ox}(E) = Q_F(E)/Q^0$, the total charge may be written as:

$$Q_T(E) = x_{Ox}(E)C_d(\sigma + E) \tag{7}$$

from which x_{Ox} can be determined. Figure 12 illustrates the values of the oxidation degree obtained from the voltammetric results following this procedure. Note that because $j_F = \nu FQ^0 dx_{Ox}/dE$, the derivative dx_{Ox}/dE vs. E is a sort of normalized faradaic voltammogram. That is, its shape must be equal to that of the faradaic response alone. So, to search if there is any capacitive current added to the faradaic current, we have simply to compare the potential dependence of x_{Ox}

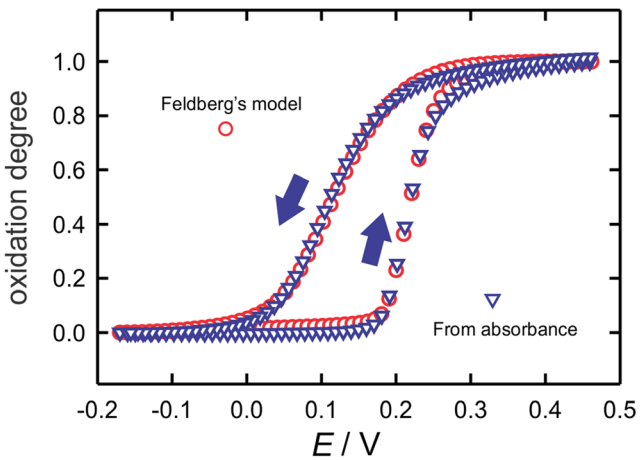

Fig. 12 Fraction of oxidized polymer as a function of the potential for Pani films in 3.7 M H_2SO_4. (o) x_{Ox} from the voltammetric results following the procedure described in the text with $C_d = 39.3$ mCV^{-1} and $\sigma = 0.403$ V. (▽) θ_{Ox} from voltabsorptiometric results. Sweep rate $v = 0.01$ Vs^{-1}. Q_T (0.45) = 3.9 mC cm^{-2}

with the potential dependence of the quotient $Q_T(E)/Q_T$ (0.45 V) [78]. A simple comparison of x_{Ox} in Fig. 12 with Q_T (E) in Fig. 11 should suffice to conclude that there are marked differences between them. Clearly, the capacitive current is present in all the potential range. Incidentally, this fact gives support to the Feldberg assumption that the capacitive current is proportional to the faradaic one [50]. Note that until the appearance of the mentioned work, there was no experimental evidence that the capacitive current was proportional to the faradaic current and therefore that the voltammetric response was the sum of both types of currents or, in other words, that the capacitive current was present from the beginning of the oxidation (also see below spectrophotometric measurements).

Soon after, Tanguy et al. [88], measuring the EIS response of Ppy, proposed a separation of capacitive and non-capacitive charge in the equivalent circuit employed to fit their results. They proposed an expression for the capacitive current of the type:

$$j_C = C_i - [1 - \exp(t/\tau) C_i](dE/dt) \quad (8)$$

where $\tau = RC$, C_i is the charging capacitance, and R is the total resistance. Their results are qualitatively fair but the pseudocapacitive current fails to go to zero as the potential increases beyond the peak. They further proposed a model in which the counterions are deep and shallow trapped near the polymer fibrils giving rise to the two types of charging.

Several further attempts of separating the capacitive and the faradaic currents have been published [75, 88–92]. Even so, there is no clear separation between the capacitive and the faradaic currents unless the final faradaic charge, Q^0, or the potential of zero charge of the polymer are evaluated by independent methods. However, we will give a brief consideration to the method proposed by Aoki et al. [93]. It is assumed that the total current, j_T, may be written as the sum of the faradaic, j_F, plus the capacitive, j_C, currents and that the latter is proportional to the faradaic charge. Then:

$$j_T = j_F + j_C \quad (9)$$

then

$$j_F(E) = j_T(E) - C\int_{Ea}^{E} j_F(u)du \quad (10)$$

The integral equation gives:

$$j_F(E) = j_T(E) - C\int_{Ea}^{E} \exp[C(E-u)] j_F(u)du \quad (11)$$

where the constant C has to be evaluated by trial and error so as to make j_F go to zero beyond certain potential. This in a way is equivalent to assume a value of Q^0 in Feldberg's model. This approach leads to asymmetrical curves for the faradaic currents.

The EIS response in the plateau region

There are numerous studies of the EIS response of Pani in acid media. However, not many of them refers to its behavior in the capacitive region and most of them are referred to a single thickness at constant pH. In general, the Nyquist plots obtained by the different workers are similar. A typical Nyquist plot for potentials in the capacitive region is shown in Fig. 13.

Inzelt et al. [94] measured the temperature of EIS response of Pani films. In the emeraldine potential region, they found results similar to those described in Fig. 13. Among other things, they found the high-frequency capacitive response to be independent of the film thickness. Similarly to Tanguy et al., they assign this capacitance to the double-layer response.

Rubinstein et al. [95] measured the EIS response of Pani films of about 150 nm in 2.0 M HCl. They found that, in the potential region corresponding to the plateau, the impedimetric response could be fitted by a capacitance in series with the solution resistance (meaning the resistance in parallel with the capacitance, that is, the charge transfer resistance, was very high).

Fiordiponti and Pistoia [96] found for Pani films of about 47 μm thick in 1 M H_2SO_4 + 0.5 M Na_2SO_4 solutions that in the potential region corresponding to the current plateau, the high-frequency capacitance gives values of about

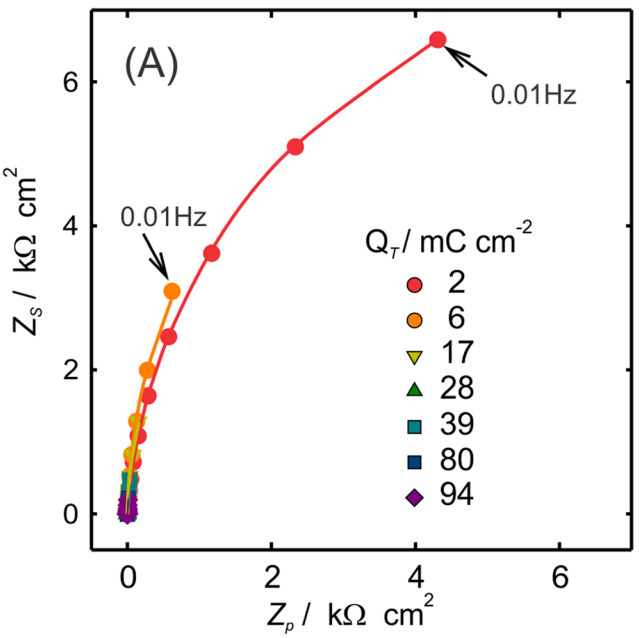

Fig. 13 Nyquist plot for Pani films of different charges Q_T (0.45) (indicated in the graphic) in 3.7 M H_2SO_4 solution. $E = 0.45$ V

10^{-1} F cm^{-2}. According to them, this high values should be attributed to a change in the extent of ion penetration and arrangement in the Pani pores. They also report that in this potential range, the Pani response tends to behave as a capacitance in series with a resistance even for relatively high frequencies. As the frequency decreases, the capacitance tends to a frequency independent value of about 0.13 F mg^{-1}, a value that agrees well with the value of 0.17 F mg^{-1} obtained by voltammetry in the plateau region.

Rosberg et al. [76] attributed the low-frequency capacitance to a series capacitance which would be the responsible of the capacitive plateau. They found it is linear with the voltammetric charge. They also found that it does not depend on the pH. They further considered that a purely capacitive-like double-layer charging is rather unlikely because of the very large surface area required to explain the very high values of the capacitance. This is based on the Feldberg estimation that a fiber radius (< 4 nm) would be required to explain a specific capacitance of 100 F cm^{-2}. They assumed that charge transfer is the responsible for the current plateau. They based in part this claim based on the fact that Kalaji and Peter [97] detected that the absorption intensity at $\lambda = 620$ nm, a wavelength attributed to polarons, increases throughout the potential range corresponding to the current peak and the current plateau. Later on, we will show that the wavelength increases in this potential range although there is no faradaic reaction.

Zic [98] studied the EIS response of Pani films in H_3PO_4 at different film thicknesses. He obtained a very good fit for an equivalent circuit formed by the series combination of two resistances in parallel with two constant phase elements (CPE). He interpreted the resistances as corresponding to an ionic charge transfer at the polymer/solution interface (R_{c1}) and as charge transfer at the bulk polymer (R_{c2}) and the corresponding CPEs (Q_{d2}) as the admittances of the double layer and the bulk polymer. The last charge transfer resistance assignation is difficult to understand since it is known that the oxidation reduction of the polymer occurs at the base metal/ polymer interface. At 0.4 V (this is just in the middle of the current plateau), R_{c2} (see Table 2 of the reference [98]) is quite big as compared with the ionic charge transfer thus suggesting that the charge transfer is much hindered at these potentials.

Popkirov and Barsoukov measured the EIS response of Ppy and polybithiophene (PBt) [99]. They claimed that, based on the experimental measurements and model simulations, they may establish the capacitive current and thus the faradaic current. From it, the authors suggest that it is this faradaic current that creates the capacitive one.

One of the problems observed with the capacitance of CPs is that the value obtained from voltammetric measurements is higher than those obtained from observed employing ac methods [80, 88, 94–96, 100–111].

To confirm this, Ren and Pickup [112] measured the capacitance in the plateau region of poly[1-methyl-3-(pyrrole-1-ylmethyl) pyridinium] films employing both voltammetry and EIS. According to these authors, although the concept of "deep trapping" proposed by Tanguy et al. for Ppy could be invoked, it is difficult to conceive it could be applied to the generality of CPs. Instead, these authors proposed that this phenomenon can be explained by the conformational changes that occur as the polymer is oxidized and reduced. As shown by Heinze and coworkers [113], in these polymers, there is a wide range of redox potential of the polymers. They arise from chain segments with different conjugation lengths leading to the fact that the oxidation potential for oxidation is higher than that for re-reduction. Thus only sites that can be oxidized and re-reduced will contribute to the current or capacitance during a cyclic potential scan. However, we think that in the capacitive current plateau potential region, there is no faradaic process and thus, this mechanism could not be operative.

Dinh and Birss [77] made an investigation on Pani films in 1 M H_2SO_4 employing large and short voltage spans as well as QCMB and EIS. They found that the capacitance was smaller during the small voltage perturbation than for large amplitudes in a similar way to that reported by Ren and Pickup [112]. Moreover, the changes of mass indicated the polymer swelling would be the reason why only some part of the oxidized polymer can be subsequently reduced. Also, these authors found they could represent the EIS results in the capacitive region by a CPE in series with a resistance. In fact, the CPE was practically a capacitance since $n \approx 0.97$.

Kalaji and Peter [97] measured the optical and electrical ac response of ITO Pani film–covered electrodes. This is an interesting approach since, in principle, the optical measurements should not be sensitive to electrons if they were the carriers within the polymer; therefore, this kind of measurements should be free of the capacitive contribution. One of the main conclusions of this work related to the capacitive contribution is that the current plateau should be attributed to a redox process in the film.

Studies comprising the measure of the epr signal and the Pauli susceptibility

Several studies about the *epr* and Pauli susceptibility changes during the oxidation of Pani, including the plateau region, have been published [114–119]. Also, the *epr* signal was measured in Ppy [120–122]. These measurements are sensitive to the presence of unpaired

electrons, and therefore, it helps to follow the course of formation of substances with these characteristics. It is well known that one of the products of the oxidation of LE are polarons the have unpaired spins. Therefore, the appearance and follow up of the *epr* signal during a potential scan should be an indication of the presence of this species.

Some time ago, it was proposed that the oxidation of leucoemeraldine (LE) leads to the formation of polarons (P), at low doping levels, which can be further oxidized to bipolarons (BP) at higher doping levels (see for instance Refs. [123–126]), as it happens with other conductive polymers such as polypyrrole and polyacetylene. This conclusion was challenged by several workers that proposed that bipolarons are generated in a first step of the oxidation and that their instability leads to the formation of polarons by an internal conversion. Finally, they separate into a polaron lattice (PL) [127, 128] that would be the species responsible for the charge transport in the polymer. However, recent spectroelectrochemical experiments strongly suggest that both Ps and BPs form at practically the same time as the polymer is oxidized (see below). All these structures are represented in Scheme 4.

Ever since, there has been many theoretical works employing more powerful methods of calculus [129–132] and including, for instance, protons and the corresponding counter ions [133]. A very useful account of more recent research is given in Ref. [132]. However, as mentioned by Bernard and Hugot-Le Goff, besides the amine, imine, and polaron sites, it is necessary to consider partially charged nitrogen atoms that do not belong exactly to these categories [134].

Genies and Lapkowski [117, 118] found that for films made and cycled in $NH_4F + 2.3$ HF, the number of spins decreases practically to zero alter the first oxidation peak. Something similar occurs in H_2SO_4 (Fig. 14).

However, for films prepared and cycled in H_2SO_4, the number of spins does not decreases after the oxidation peak, in agreement with previous findings in this media [114–116]. This also seems to be in agreement with recent spectroelectrochemical experiments (see below and Ref. [78]). On the other hand, these authors propose for Pani, in similitude to Ppy, that polarons are first formed at lower potentials and then bipolarons are formed. This is a variance with latter views in the sense that, for Pani, bipolarons seems to be less stable that the polaron lattice [127]. Later on, the same authors studied the influence of different anions on the shape of the *epr* spectra [118] They conclude that the interaction with the positive charges change the nature of the polyaniline spins and propose that, based on a previous model of Epstein and MacDiarmid [135], at low potentials (before the voltammetric peak), there are Curie spins that, on further increase of the potential, aggregate into metallic islands that respond as the Pauli spins.

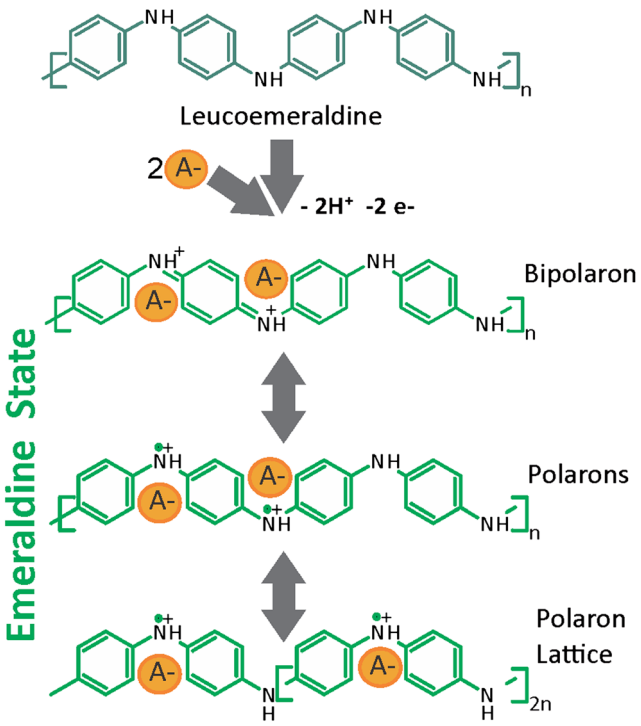

Scheme 4 Structures of leucoemeraldine base and emeraldine salt in its different forms: bipolarons, polarons, and polaron lattice

Spectroelectrochemical studies UV-vis

There are many studies of the UV-vis spectra of Pani (see Refs. [43, 123, 124, 136–140], just to quote a few). However, only a few of them contains information about the capacitive current during the oxidation of the polymer. For the

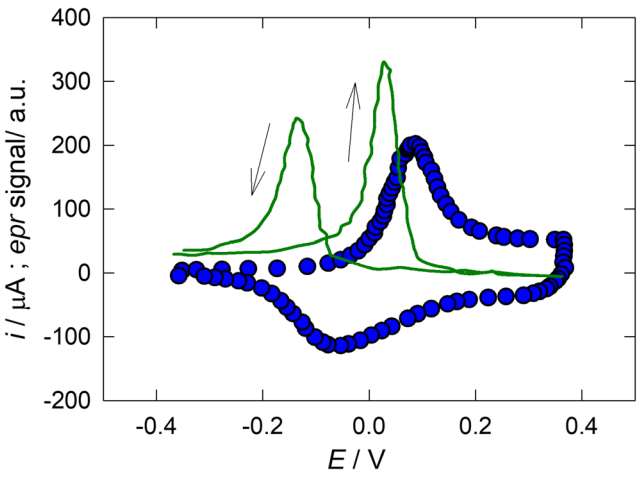

Fig. 14 Voltammogram (•) and epr number of spins (—) of a Pani film (20 mC) in 1 M H_2SO_4, prepared in 35% HBF_4 $v = 0.01$ V s^{-1}. Potentials referred to a silver wire pseudo-reference electrode. Redrawn from data of Ref. [118]

sake of reference, we show the spectra of Pani free-standing films at a few different fixed applied potentials (Fig. 15). This brief presentation of the spectral characteristics of Pani is based on a previous publication [78].

In Fig. 15, there is a band centered at 320 nm that decreases as the potential increases; this means that the species responsible of that absorption band disappears as the polymer is oxidized. Other two bands at about 400 nm and 750 nm increase with the potential. Actually, it was found that the band at 400 nm was composed of at least two bands: one peaking at about 390 nm and another around 440 nm.

In the potential range comprised between − 0.2 V and 0.3 V, there are three isosbestic points generated by the potential change and they refer to an electrochemical equilibrium between the reduced and oxidized Pani. Outside the potential range where the faradaic reaction occurs, there is another crossing point that should not involve an electrochemical (Nernstian) equilibrium but rather other type of potential dependence [78].

Also, experiments sweeping the potential at fixed wavelengths have been done [43, 78, 137] (see Fig. 16).

In the potential range in which the faradaic process occurs, the traces of the anodic sweep at the three wavelengths are similar in shape (Fig. 16). In the potential region corresponding to the purely capacitive response, as noted by previous workers [43, 137], the absorbance at 400 nm linearly decreases with the potential, whereas the absorbance at 750 nm increases. There is general consensus about the species absorbing at 750–800 nm being the PL, whereas those absorbing at 440 nm are BPs [139]. The fact that the absorbance at 320 remains approximately constant in this region means that the optical oxidation degree, θ_{Ox}, could be approximately estimated as:

$$\theta_{Ox} = \frac{A_{0.45} - A(E)}{A_{0.45} - A_{-0.20}} = \frac{A(E) - A_{-0.20}}{\Delta A_T} \quad (12)$$

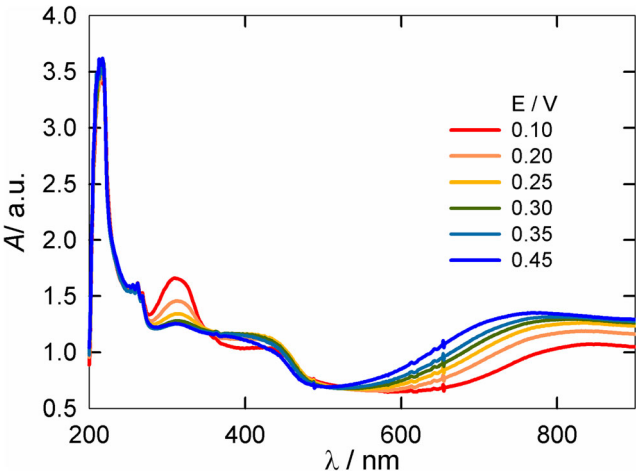

Fig. 15 UV-visible spectra of a free-standing membrane of Pani in H_2SO_4 solutions at different applied potentials. $Q_T = 50$ mC cm^{-2}

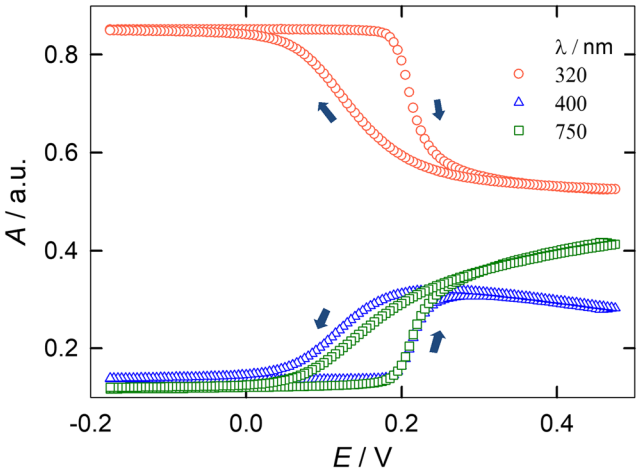

Fig. 16 Absorbance as a function of potential for a Pani film deposited on ITO in 3.7 M H_2SO_4 solution [78], at different wavelengths. $v = 0.005$ Vs^{-1}. $Q_T = 5$ mC cm^{-2}

where $A(E)$ is the absorbance at potential E, $A_{0.45}$, the absorbance at $E = 0.45$ V, $A_{-0.20}$, the absorbance at $E = -0.20$ V, and $\Delta A_T = A_{-0.20} - A_{0.45}$, the total absorbance change in going from the completely reduced polymer film, $E = -0.20$ V, to the half oxidized polymer film, $E = 0.45$ V. The values of θ_{Ox} as a function of E obtained in this way are shown in Fig. 12.

Measurements of the in situ conductivity

Since we are interested here about the nature of the capacitive currents and if this is caused by an electrical double layer, the problem is related to the conductivity of Pani and to the nature of the current carriers in the polymer.

Although we refer to the conductivity, what was really measured is the resistance since in most cases, it is difficult to define precisely the thickness or the area or both. An exact method was proposed and employed by Kankare [141]. There are several reports about the in situ resistance of Pani. The resistance of emeraldine has received much attention. Studies of the conductivity changes of the neutral form of polyaniline upon protonation have been made [115, 142, 143]. Also, the effect of the anion present with the emeraldine salt has been measured [72]. The mechanism of conduction of emeraldine has been studied as a function of temperature jointly with EPR measurements [144]. There are several studies of the conductivity of many copolymers and blends of Pani with other materials. However, there are very few studies of the in situ changes of conductivity of Pani as it is oxidized from the leucoemeraldine (LE) form to the E form [145–148]. Also, the conductivity of Pani has been measured for nanowires [149] and hepta-aniline oligomers [150].

The potential dependence of the logarithm of the inverse of the resistance is shown in Fig. 17.

The resemblance of Fig. 17 with Fig. 12 strongly suggest there must be a close relationship between the conductivity of the polymer, σ, and the fraction of oxidized redox sites x_{Ox}. On the other hand, it is interesting to note that the conductivity steadily increases as the potential increases, thus showing that the carriers are formed as soon as the oxidation begins. This remark is opposite to the suggestions that carriers are formed at the expensed of species formed at the beginning of the oxidation of the LE.

About the nature and origin of the capacitance in Pani

In acid solutions, the conductivity of the Pani increases as the polymer is oxidized [71, 145–147] and has a maximum value at about 0.45 V (SCE). Although most of the works show a good agreement between the calculated and the experimental data for the band assignation to the different species of Pani, there is still no consensus about how many chemically different species form as products of the oxidation of leucoemeraldine, and which ones are the carriers, that is, the species actually responsible for the charge transport and the capacitance of the polymer. Moreover, other workers associate the conductivity of Pani with electrons and trapped ions [151–153]. If the double-layer charging were associated to free electrons, i.e., the conduction mechanism was like in a metal; they would not be seen in the absorbance measurements. It has been shown recently that the double-layer charging is related to the increase of the absorbance 750 nm (mainly associated to the PL). As the potential is increased in this range, the amount of carriers required to charge the double layer is provided by a displacement of the equilibrium BP ↔ PL in favor of the latter. This is in agreement with Barsukov and Chivikov [79] that suggested that the formation of a PL is related to the charging of the double layer.

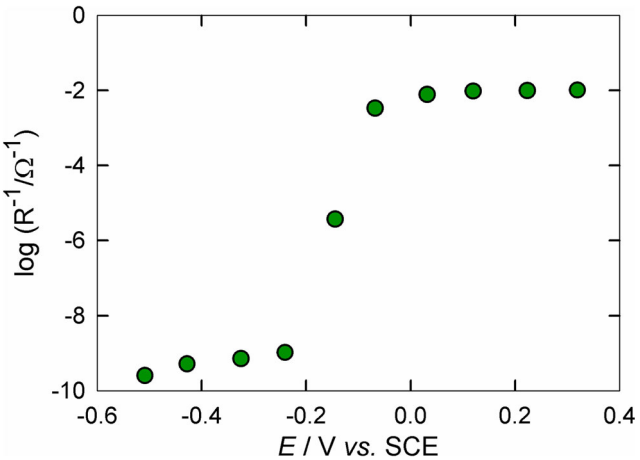

Fig. 17 Semi-logarithmic plot of the inverse of the resistance as a function of the applied potential. The potentials are referred to the scale of SCE in aqueous solutions. Data taken from Wrighton et al. [146]

Influence of the nature of the electrolyte and the pH on j_{cap}

Although there is a large amount of work devoted to the influence of the pH and the nature of present anions on the synthesis and redox switching of Pani, not much attention has been paid to this influence on the capacitive currents. One of the first studies on the influence of the anion on j_{cap} is that of Genies et al.'s. [75]. In this work, j_{cap} increases in the order $ClO_4^- < Cl^- < HSO_4^-$. On the other hand, Barbero et al. found, employing the probe beam deflection (PBD), that the signal at 0.7 V (vs. RHE) in HCl increased as the acid concentration decreased from 4 to 0.1 M. Similarly, they found, in similar conditions, that the PBD signal increases in the order $ClO_4^- < Cl^- < HSO_4^-$ [64]. Moreover, Hu et al. showed a similar sequence of the electrolytes with increasing mean capacitance for Pani-coated electrodes: $CCl_3COOH <$ $< HCl < H_2SO_4$ [154].On the other hand, Lizarraga et al. [155, 156] measured the volume changes of Pani in different electrolytes. Their results are assembled in Table 1.

Few studies of the influence of the *pH* on j_{cap} exist in the literature. Care should be taken when comparing j_{cap} at different pH values at the same applied potential because of the cathodic shift of the peak potential with the pH in the range $-1.0 < pH < 2.0$. Moreover as the pH increases, another anodic process appears in the capacitive region and the current increases [70]. Scotto et al. showed that no dependence of the capacitive current in this pH range appears in constant ionic strength solutions of $H_2SO_4 + Na_2SO_4$, $HCl + NaCl$, and $HClO_4 + NaClO_4$. However, Genies et al. [75] reported an increase of j_{cap} of the order of 24% for H_2SO_4 solutions when sweeping the potential between 0.38 and 0.40 V.

EQCM has been also employed to study the ion exchange accompanying the faradaic and capacitive current responses. Although the detailed analysis of the EQCM response associated to the redox commutation of Pani reveals a complex behavior [157], Inzelt stressed the differences between redox and conducting polymers in the capacitive region: whereas for redox polymers the ion exchange stops (a mass plateau is reached) after the faradaic process in the anodic scan, the ion sorption continues (and the mass linearly increases with potential in the capacitive region) after the anodic peak in the case of Pani [158]. This effect was ascribed to the double-layer charging phenomenon. In this sense, Pruneanu et al. made an electrochemical quartz crystal microbalance study of the behavior of Pani in $HClO_4$, 4-toluenesulfonic, and 5-sulfosalicylic acid solutions [159]. They concluded that the relative participation of

Table 1 Relative volume changes, $\Delta V/V$, of Pani in different electrolytes

Electrolyte	$HClO_4$	H_2SO_4	HCl
4 M	0.016	0.032	0.035
1 M	0.030	0.050	0.055

protons and anions in the ion exchange processes is determined by the pH of the solution. They also concluded that in the presence of large anions, the film structure becomes open.

Recapitulation

From the foregoing text, it is evident that there are many models to explain the nature of the capacitance in Pani. We can state that there has been (and there still is) a controversy about the nature of this capacitance. Some authors sustain that it is due to an electrochemical reaction whereas many others believe it is a double-layer process. However, arguments in favor of the latter are very strong. Many of the observed experimental facts may be explained considering that the current observed in the plateau region is double-layer type and not a pseudocapacitive process.

Firstly, there seems to be agreement that the voltammetric peak is due to a reversible confined electrochemical process with interaction among the redox centers, and therefore, once it is finished, the faradaic current should become zero. The spectroelectrochemical evidence suggests that this scheme seems to be true. Proof of that is obtained from the coincidence of the voltammetric oxidation degree, calculated from Feldberg's model, and the spectroelectrochemical oxidation degree obtained from the decrease of the band at 320 nm. This would confirm the model proposed by Feldberg in the sense that the current at the plateau is proportional to the amount of polymer oxidized. Also it implies that *the capacitive and faradaic currents cannot be separated* from voltammetric measurements without extra assumptions.

Moreover, the EIS response of Pani in the plateau region seems to indicate that the interface at the polymer fibrils/internal solution interface may be represented by an equivalent circuit consisting of a capacitance in parallel with a high charge transfer resistance. It is interesting to point out that the capacitances in the plateau region determined by voltammetry and EIS are very similar. Furthermore, from the spectroelectrochemical evidence, it seems that PLs are the carriers and the observed double-layer capacitance is due to an accumulation or depletion of them at the polymer fibrils/internal solution interface.

Acknowledgments WAM and DP are members of the CIC of the CONICET. JS thanks a fellowship from CONICET.

Funding information This work was financially supported by the Consejo Nacional de Investigaciones Científicas y Técnicas (CONICET) (PIP 0813), the Agencia Nacional de Promoción Científica Tecnológica (ANPCyT) (PICT-0407, PICT-2015-0239), and the Universidad Nacional de La Plata (UNLP) (PPID-X016).

References

1. Conway BE (1999) Electrochemical supercapacitors: scientific fundamentals and technological applications. Springer
2. Eftekhari A, Li L, Yang Y (2017) Polyaniline supercapacitors. J Power Sources 347:86–107. https://doi.org/10.1016/j.jpowsour.2017.02.054
3. Liu J, Zhou M, Fan L-Z et al (2010) Porous polyaniline exhibits highly enhanced electrochemical capacitance performance. Electrochim Acta 55:5819–5822. https://doi.org/10.1016/j.electacta.2010.05.030
4. Zhou K, He Y, Xu Q et al (2018) A hydrogel of ultrathin pure polyaniline nanofibers: oxidant-templating preparation and supercapacitor application. ACS Nano 12:5888–5894. https://doi.org/10.1021/acsnano.8b02055
5. Guan H, Fan L-Z, Zhang H, Qu X (2010) Polyaniline nanofibers obtained by interfacial polymerization for high-rate supercapacitors. Electrochim Acta 56:964–968. https://doi.org/10.1016/j.electacta.2010.09.078
6. Miao Y, Fan W, Chen D, Liu T (2013) High-performance supercapacitors based on hollow polyaniline nanofibers by electrospinning. ACS Appl Mater Interfaces 5:4423–4428. https://doi.org/10.1021/am4008352
7. Sydulu SB, Palaniappan S, Srinivas P (2013) Nano fibre polyaniline containing long chain and small molecule dopants and carbon composites for supercapacitor. Electrochim Acta 95:251–259. https://doi.org/10.1016/j.electacta.2013.02.040
8. Ghenaatian HR, Mousavi MF, Rahmanifar MS (2012) High performance hybrid supercapacitor based on two nanostructured conducting polymers: self-doped polyaniline and polypyrrole nanofibers. Electrochim Acta 78:212–222. https://doi.org/10.1016/j.electacta.2012.05.139
9. Wang K, Huang J, Wei Z (2010) Conducting polyaniline nanowire arrays for high performance supercapacitors. J Phys Chem C 114:8062–8067
10. He S, Hu X, Chen S et al (2012) Needle-like polyaniline nanowires on graphite nanofibers: hierarchical micro/nano-architecture for high performance supercapacitors. J Mater Chem 22:5114. https://doi.org/10.1039/c2jm15668g
11. Dhawale DS, Vinu A, Lokhande CD (2011) Stable nanostructured polyaniline electrode for supercapacitor application. Electrochim Acta 56:9482–9487. https://doi.org/10.1016/j.electacta.2011.08.042
12. Chen W, Rakhi RB, Alshareef HN (2013) Facile synthesis of polyaniline nanotubes using reactive oxide templates for high energy density pseudocapacitors. J Mater Chem A 1:3315. https://doi.org/10.1039/c3ta00499f
13. Marmisollé WA, Azzaroni O (2016) Recent developments in the layer-by-layer assembly of polyaniline and carbon nanomaterials for energy storage and sensing applications. From synthetic aspects to structural and functional characterization. Nanoscale 8:9890–9918. https://doi.org/10.1039/C5NR08326E
14. Blighe FM, Diamond D, Coleman JN, Lahiff E (2012) Increased response/recovery lifetimes and reinforcement of polyaniline nanofiber films using carbon nanotubes. Carbon N Y 50:1447–1454. https://doi.org/10.1016/j.carbon.2011.10.022
15. Du X, Liu H-Y, Cai G et al (2012) Use of facile mechanochemical method to functionalize carbon nanofibers with nanostructured polyaniline and their electrochemical capacitance. Nanoscale Res Lett 7:111. https://doi.org/10.1186/1556-276X-7-111
16. Wang K, Meng Q, Zhang Y et al (2013) High-performance two-ply yarn supercapacitors based on carbon nanotubes and polyaniline nanowire arrays. Adv Mater 25:1494–1498. https://doi.org/10.1002/adma.201204598

17. Chen S, Hu Y, Li Z et al (2017) High-performance supercapacitors based on electrochemical-induced vertical-aligned carbon nanotubes and polyaniline nanocomposite electrodes. Sci Rep 7:1–8. https://doi.org/10.1038/srep43676
18. Zhang K, Zhang LL, Zhao XS, Wu J (2010) Graphene/polyaniline nanofiber composites as supercapacitor electrodes. Chem Mater 22:1392–1401. https://doi.org/10.1021/cm902876u
19. Li X, Song H, Zhang Y et al (2012) Enhanced electrochemical capacitance of graphene nanosheets coating with polyaniline for supercapacitors. Int J Electrochem Sci 7:5163–5171
20. Li L, Raji A-RO, Fei H et al (2013) Nanocomposite of polyaniline nanorods grown on graphene nanoribbons for highly capacitive pseudocapacitors. ACS Appl Mater Interfaces 5:6622–6627. https://doi.org/10.1021/am4013165
21. Basnayaka PA, Ram MK, Stefanakos EK, Kumar A (2013) Supercapacitors based on graphene-polyaniline derivative nanocomposite electrode materials. Electrochim Acta 92:376–382. https://doi.org/10.1016/j.electacta.2013.01.039
22. Fenoy GE, Van der Schueren B, Scotto J et al (2018) Layer-by-layer assembly of iron oxide-decorated few-layer graphene/PANI: PSS composite films for high performance supercapacitors operating in neutral aqueous electrolytes. Electrochim Acta 283:1178–1187. https://doi.org/10.1016/j.electacta.2018.07.085
23. Gao Z, Yang W, Wang J et al (2013) Electrochemical synthesis of layer-by-layer reduced graphene oxide sheets/polyaniline nanofibers composite and its electrochemical performance. Electrochim Acta 91:185–194. https://doi.org/10.1016/j.electacta.2012.12.119
24. Kumar NA, Choi H, Shin YR et al (2012) Polyaniline-grafted reduced graphene oxide for efficient electrochemical supercapacitors. ACS Nano 6:1715–1723
25. Wu J, Zhang Q, Wang J et al (2018) A self-assembly route to porous polyaniline/reduced graphene oxide composite materials with molecular-level uniformity for high-performance supercapacitors. Energy Environ Sci 11:1280–1286. https://doi.org/10.1039/C8EE00078F
26. Li P, Zhang D, Xu Y et al (2018) Hierarchical porous polyaniline supercapacitor electrode from polyaniline/silica self- aggregates. Polym Int 67:1670–1676. https://doi.org/10.1002/pi.5692
27. Li X, Chai Y, Zhang H et al (2012) Synthesis of polyaniline/tin oxide hybrid and its improved electrochemical capacitance performance. Electrochim Acta 85:9–15. https://doi.org/10.1016/j.electacta.2012.07.124
28. Iranagh SA, Eskandarian L, Mohammadi R (2013) Synthesis of MnO2-polyaniline nanofiber composites to produce high conductive polymer. Synth Met 172:49–53. https://doi.org/10.1016/j.synthmet.2013.04.002
29. de Levie R (1990) Fractals and rough electrodes. J Electroanal Chem Interfacial Electrochem 281:1–21. https://doi.org/10.1016/0022-0728(90)87025-F
30. Bard AJ, Faulkner LR (2001) Electrochemical methods. Fundamentals and applications, 2nd edn. Wiley, USA
31. van den Eeden ALG, Sluyters JH, van Lenthe JH (1984) The metal side of the electrical double layer at the metal/electrolyte interface. J Electroanal Chem Interfacial Electrochem 171:195–217. https://doi.org/10.1016/0022-0728(84)80114-X
32. Grahame DC (1947) The electrical double layer and the theory of electrocapillarity. Chem Rev 41:441–501. https://doi.org/10.1021/cr60130a002
33. Hamelin A (1985) Double-layer properties at sp and sd metal single-crystal electrodes. Mod Asp Electrochem
34. Vorotyntsev MA (1986) Modern state of double layer study of solid metals. In: Mod. Asp. Electrochem, pp 131–222
35. Plieth WJ, Vetter KJ (1968) Thermodynamik der Phasengrenze Metall/Elektrolyt reversibler Elektroden. Ber Bunsenges Phys Chem 72:673–680. https://doi.org/10.1002/bbpc.19680720604
36. Frumkin A, Petry O, Damaskin B (1970) The notion of the electrode charge and the Lippmann equation. J Electroanal Chem Interfacial Electrochem 27:81–100. https://doi.org/10.1016/S0022-0728(70)80204-2
37. Marmisolle WA, Capdevila DA, De LE et al (2013) Self-assembled monolayers of NH2-terminated thiolates: order, pKa, and specific adsorption. Langmuir 29:5351–5359
38. Conway BE (1965) Theory and principles of electrode processes. Ronald Press Co
39. Brown AP, Anson FC (1977) Cyclic and differential pulse voltammetric behavior of reactants confined to the electrode surface. Anal Chem 49:1589–1595. https://doi.org/10.1021/ac50019a033
40. Clark A (1970) Theory of adsorption and catalysis
41. Srinivasan S, Gileadi E (1966) The potential-sweep method: a theoretical analysis. Electrochim Acta 11:321–335. https://doi.org/10.1016/0013-4686(66)87043-3
42. Diaz a F, Castillo JI, Logan JA, Lee W-Y (1981) Electrochemistry of conducting polypyrrole films. J Electroanal Chem Interfacial Electrochem 129:115–132. https://doi.org/10.1016/S0022-0728(81)80008-3
43. Kobayashi T, Yoneyama H, Tamura H (1984) Electrochemical reactions concerned with electrochromism of polyaniline film-coated electrodes. J Electroanal Chem 177:281–291. https://doi.org/10.1016/0022-0728(84)80229-6
44. Waltman RJ, Bargon J, Diaz AF (1983) Electrochemical studies of some conducting polythiophene films. J Phys Chem 87:1459–1463. https://doi.org/10.1021/j100231a035
45. Marmisollé WA, Florit MI, Posadas D (2011) A formal representation of the anodic voltammetric response of polyaniline. J Electroanal Chem 655:17–22. https://doi.org/10.1016/j.jelechem.2011.02.019
46. Albuquerque J, Mattoso LH, Balogh D et al (2000) A simple method to estimate the oxidation state of polyanilines. Synth Met 113:19–22. https://doi.org/10.1016/S0379-6779(99)00299-4
47. Kang E, Neoh KG, Tan KL (1998) Polyaniline: a polymer with many interesting intrinsic redox states. Prog Polym Sci 23:277–324. https://doi.org/10.1016/S0079-6700(97)00030-0
48. Kalaji M, Peter LM, Abrantes LM, Mesquita JC (1989) Microelectrode studies of fast switching in polyaniline films. J Electroanal Chem Interfacial Electrochem 274:289–295. https://doi.org/10.1016/0022-0728(89)87051-2
49. Marmisollé WA, Florit MI, Posadas D (2013) Coupling between proton binding and redox potential in electrochemically active macromolecules. The example of polyaniline. J Electroanal Chem 707:43–51. https://doi.org/10.1016/j.jelechem.2013.08.012
50. Scotto J, Florit MI, Posadas D (2017) pH dependence of the voltammetric response of polyaniline. J Electroanal Chem 785:14–19. https://doi.org/10.1016/j.jelechem.2016.11.066
51. Marmisollé WA, Florit MI, Posadas D (2014) Acid-base equilibrium in conducting polymers. The case of reduced polyaniline. J Electroanal Chem. https://doi.org/10.1016/j.jelechem.2014.03.003
52. Doblhofer K, Vorotyntsev M (1994) The membrane properties of electroactive polymer films. In: Electroact. Polym. Electrochem. Springer US, Boston, MA, pp 375–442
53. Andrade EM, Molina V, Florit I, Posadas D (2000) Volume changes of poly (2-methylaniline) upon redox switching. Electrochem Solid-State Lett 3:504–507
54. Horányi G, Inzelt G (1988) Application of radiotracer methods to the study of the formation and behaviour of polymer film electrodes. Investigation of the formation and overoxidation of labelled polyaniline films. J Electroanal Chem 257:311–317. https://doi.org/10.1016/0022-0728(88)87052-9
55. Kazarinov VE, Andreev VN, Spytsin MA, Shlepakov AV (1990) Role of anions in the electrochemical transformation processes of

polyaniline. Electrochim Acta 35:899–904. https://doi.org/10.1016/0013-4686(90)90087-G
56. Orata D, Buttry DA (1987) Determination of ion populations and solvent content as functions of redox state and pH in polyaniline. J Am Chem Soc 109:3574–3581. https://doi.org/10.1021/ja00246a013
57. Daifuku H, Kawagoe T, Yamamoto N et al (1989) A study of the redox reaction mechanisms of polyaniline using a quartz crystal microbalance. J Electroanal Chem Interfacial Electrochem 274:313–318. https://doi.org/10.1016/0022-0728(89)87054-8
58. Sapoval B, Gutfraind R, Meakin P et al (1993) Equivalent-circuit, scaling, random-walk simulation, and an experimental study of self-similar fractal electrodes and interfaces. Phys Rev E 48:3333–3344. https://doi.org/10.1103/PhysRevE.48.3333
59. Cordoba-Torresi S, Gabrielli C, Keddam M et al (1990) Role of ion exchange in the redox processes of a polyaniline film studied by an ac quartz crystal microbalance. J Electroanal Chem Interfacial Electrochem 290:269–274. https://doi.org/10.1016/0022-0728(90)87437-O
60. Bácskai J, Kertész V, Inzelt G (1993) An electrochemical quartz crystal microbalance study of the influence of pH and solution composition on the electrochemical behaviour of poly(aniline) films. Electrochim Acta 38:393–397. https://doi.org/10.1016/0013-4686(93)85156-S
61. Ramirez S, Hillman AR (1998) Electrochemical quartz crystal microbalance studies of poly(ortho-toluidine) films exposed to aqueous Perchloric acid solutions. J Electrochem Soc 145:2640. https://doi.org/10.1149/1.1838693
62. Andrade E, Molina F, Florit M, Posadas D (1996) IR response of poly (o-toluidine): spectral modifications upon redox state change. J Electroanal Chem 419:15–21
63. Troise Frank MH, Denuault G (1994) Scanning electrochemical microscope (SECM) study of the relationship between proton concentration and electronic charge as a function of ionic strength during the oxidation of polyaniline. J Electroanal Chem 379:399–406. https://doi.org/10.1016/0022-0728(94)87163-9
64. Barbero C, Miras MC, Haas O, Kotz R (1991) Alteration of the ion exchange mechanism of an electroactive polymer by manipulation of the active site probe beam deflection and quartz crystal ~ crobal ~~ e study of poly @ niline and poly (Wmethylaniline). J Electroanal Chem 310:437–443
65. Shimazu K, Murakoshi K, Kita H (1990) Quantitative and in-situ measurements of proton transport at polyaniline film electrodes. J Electroanal Chem Interfacial Electrochem 277:347–353. https://doi.org/10.1016/0022-0728(90)85114-K
66. Lapkowski M, Genies EM (1990) Spectroelectrochemical studies of proton exchange processes in the electrochemical reactions of polyaniline using pH indicators. J Electroanal Chem Interfacial Electrochem 284:127–140. https://doi.org/10.1016/0022-0728(90)87067-T
67. Ybarra G, Moina C, Florit MI, Posadas D (2000) Proton exchange during the redox switching of polyaniline film electrodes. Electrochem Solid-State Lett 3:330–332. https://doi.org/10.1149/1.1391139
68. Baba A, Tian S, Stefani F et al (2004) Electropolymerization and doping/dedoping properties of polyaniline thin films as studied by electrochemical-surface plasmon spectroscopy and by the quartz crystal microbalance. J Electroanal Chem 562:95–103. https://doi.org/10.1016/j.jelechem.2003.08.012
69. Scotto J, Florit MI, Posadas D (2016) The effect of membrane equilibrium on the behaviour of electrochemically active polymers. J Electroanal Chem 774:42–50. https://doi.org/10.1016/j.jelechem.2016.04.052
70. Scotto J, Florit MI, Posadas D (2018) Redox commuting properties of polyaniline in hydrochloric, sulphuric and perchloric acid solutions. J Electroanal Chem 817:160–166. https://doi.org/10.1016/j.jelechem.2018.03.057
71. Focke WW, Wnek GE, Wei Y (1987) Influence of oxidation state, pH, and counterion on the conductivity of polyaniline. J Phys Chem 91:5813–5818. https://doi.org/10.1021/j100306a059
72. Saraswathi R, Kuwabata S, Yoneyama H (1992) Influence of basicity of dopant anions on the conductivity of polyaniline. J Electroanal Chem 335:223–231. https://doi.org/10.1016/0022-0728(92)80244-X
73. MacDiarmid AG, Epstein AJ (1995) Secondary doping in polyaniline. Synth Met 69:85–92. https://doi.org/10.1016/0379-6779(94)02374-8
74. Lee K-H, Park BJ, Song DH et al (2009) The role of acidic m-cresol in polyaniline doped by camphorsulfonic acid. Polymer (Guildf) 50:4372–4377. https://doi.org/10.1016/j.polymer.2009.07.009
75. Genies EM, Penneau JF, Vieil E (1990) The influence of counteranions and pH on the capacitive current of conducting polyaniline. J Electroanal Chem 283:205–219
76. Roßberg K, Paasch G, Dunsch L, Ludwig S (1998) The influence of porosity and the nature of the charge storage capacitance on the impedance behaviour of electropolymerized polyaniline films. J Electroanal Chem 443:49–62. https://doi.org/10.1016/S0022-0728(97)00494-4
77. Dinh HN, Birss VI (1998) Electrochemical and mass measurements during small voltage amplitude perturbations of conducting polyaniline films. J Electroanal Chem 443:63–71. https://doi.org/10.1016/S0022-0728(97)00470-1
78. Scotto J, Florit MI, Posadas D (2018) About the species formed during the electrochemical half oxidation of polyaniline: polaron-bipolaron equilibrium. Electrochim Acta 268:187–194. https://doi.org/10.1016/j.electacta.2018.02.066
79. Barsukov V, Chivikov S (1996) The “capacitor” concept of the current-producing process mechanism in polyaniline type conducting polymers. Electrochim Acta 41:1773–1779. https://doi.org/10.1016/0013-4686(95)00494-7
80. Kalaji M, Peter L (1982) No title. J Chem Soc Faraday Trans 129:853
81. Feldberg SW (1984) Reinterpretation of polypyrrole electrochemistry. Consideration of capacitive currents in redox switching of conducting polymers. J Am Chem Soc 106:4671–4674. https://doi.org/10.1021/ja00329a004
82. Huang W-S, Humphrey BD, MacDiarmid AG (1986) Polyaniline, a novel conducting polymer. Morphology and chemistry of its oxidation and reduction in aqueous electrolytes. J Chem Soc, Faraday Trans 1 F 88:2385–2400
83. Munakata H, Oyamatsu D, Kuwabata S (2004) Effects of omega-functional groups on pH-dependent reductive desorption of alkanethiol self-assembled monolayers. Langmuir 20:10123–10128. https://doi.org/10.1021/la048878h
84. Kalaji M, Nyholm L, Peter LM (1991) A microelectrode study of the influence of pH and solution composition on the electrochemical behaviour of polyaniline films. J Electroanal Chem 313:271–289. https://doi.org/10.1016/0022-0728(91)85185-R
85. Genies EM, Boyle A, Lapkowski M, Tsintavis C (1990) Polyanilne: a historical survey. Synth Met 36:139–182
86. Rudzinski WE, Lozano L, Walker M (1990) The effects of pH on the polyaniline switching reaction. J Electrochem Soc 137:3132. https://doi.org/10.1149/1.2086172
87. Inzelt G, Horányi G (1990) Some problems connected with the study and evaluation of the effect of pH and electrolyte

concentration on the behaviour of polyaniline film electrodes. Electrochim Acta 35:27–34. https://doi.org/10.1016/0013-4686(90)85032-I
88. Tanguy J, Mermilliod N, Hoclet M (1987) Capacitive charge and noncapacitive charge in conducting polymer electrodes. J Electrochem Soc 134:795–802. https://doi.org/10.1149/1.2100575
89. Servagent S, Vieil E (1989) Resistance and differential capacitance of poly(3-methylthiophene) films. Comparison between cyclic voltammetry and chronopotentiometry. Synth Met 31:127–139
90. Matencio T, Vieil E (1991) Variable capacitance and conductance in polyaniline: a simple model with interacting sites and a single quasi-reversible charge transfer. Synth Met 43:3001–3004
91. Vorotyntsev MA, Daikhin LI, Levi MD (1992) Isotherms of electrochemical doping and cyclic voltammograms of electroactive polymer films. J Electroanal Chem 332:213–235
92. Aoki K, Cao J, Hoshino Y (1993) Coulombic irreversibility at polyaniline-coated electrodes by electrochemical switching. Electrochim Acta 38:1711–1716. https://doi.org/10.1016/0013-4686(93)85066-8
93. Tezuka Y, Aoki K, Shinozaki K (1989) Kinetics of oxidation of polypyrrole-coated transparent electrodes by in situ linear sweep voltammetry and spectroscopy. Synth Met 30:369–379. https://doi.org/10.1016/0379-6779(89)90660-7
94. Inzelt G, Láng G, Kertész V, Bácskai J (1993) Effect of the temperature on the conductivity and capacitance of poly(aniline) film electrodes. Electrochim Acta 38:2503–2510. https://doi.org/10.1016/0013-4686(93)80145-P
95. Rubinstein I, Sabatani E, Rishpon J (1987) Electrochemical impedance analysis of polyaniline films on electrodes. J Electrochem Soc 134:3078–3083. https://doi.org/10.1149/1.2100343
96. Fiordiponti P, Pistoia G (1989) An impedance study of polyaniline films in aqueous and organic solutions. Electrochim Acta 34:215–221. https://doi.org/10.1016/0013-4686(89)87088-4
97. Kalaji M, Peter LM (1991) Optical and electrical a.c. response of polyaniline films. J Chem Soc Faraday Trans 87:853–860. https://doi.org/10.1039/FT9918700853
98. Žic M (2007) The effect of the PANI-free volume on impedance response. J Electroanal Chem 610:57–66. https://doi.org/10.1016/j.jelechem.2007.07.001
99. Popkirov GS, Barsoukov E (1995) In-situ impedance measurements during oxidation and reduction of conducting polymers: significance of the capacitive currents. J Electroanal Chem 383:155–160
100. Naoi K, Lien MM, Smyrl WH, Owens BB (1989) Capacitive behavior in conducting polymers. Appl Phys Commun 9:14
101. Pickup PG (1990) Alternating current impedance study of a polypyrrole-based anion-exchange polymer. J Chem Soc Faraday Trans 86:3631–3636. https://doi.org/10.1039/FT9908603631
102. Ren X, Pickup PG (1992) Ionic and electronic conductivity of poly-(3-methylpyrrole-4-carboxylic acid). J Electrochem Soc 139:2097–2105. https://doi.org/10.1149/1.2221185
103. Grzeszczuk M, Żabińska-Olszak G (1993) Ionic transport in polyaniline film electrodes: an impedance study. J Electroanal Chem 359:161–174. https://doi.org/10.1016/0022-0728(93)80407-9
104. Komura T, Sakabayashi H, Takahashi K (1995) Electrochemical impedance study and characteristics of polyaniline film electrodes. Bull Chem Soc Jpn 68:476–480. https://doi.org/10.1246/bcsj.68.476
105. Genz O, Lohrengel MM, Schultze JW (1994) Potentiostatic pulse and impedance investigations of the redox process in polyaniline films. Electrochim Acta 39:179–185. https://doi.org/10.1016/0013-4686(94)80053-7
106. Sandí G, Vanýsek P (1994) Impedance and voltammetric studies of electrogenerated polyaniline conducting films. Synth Met 64:1–8. https://doi.org/10.1016/0379-6779(94)90266-6
107. Mermilliod N, Tanguy J, Petiot F (1986) A study of chemically synthesized polypyrrole as electrode material for battery applications. J Electrochem Soc 133:1073. https://doi.org/10.1149/1.2108788
108. Tanguy J, Slama M, Hoclet M, Baudouin JL (1989) Impedance measurements on different conducting polymers. Synth Met 28:145–150. https://doi.org/10.1016/0379-6779(89)90512-2
109. Tanguy J, Baudoin JL, Chao F, Costa M (1992) Study of the redox mechanism of poly-3-methylthiophene by impedance spectroscopy. Electrochim Acta 37:1417–1428. https://doi.org/10.1016/0013-4686(92)87016-S
110. Tanguy J, Proń A, Zagórska M, Kulszewicz-Bajer I (1991) Poly(3-alkylthiophenes) and poly(4,4′-dialkyl-2,2′-bithiophenes): a comparative study by impedance spectroscopy and cyclic voltammetry. Synth Met 45:81–105. https://doi.org/10.1016/0379-6779(91)91849-6
111. Feldman BJ, Burgmayer P, Murray RW (1985) The potential dependence of electrical conductivity and chemical charge storage of poly(pyrrole) films on electrodes. J Am Chem Soc 107:872–878. https://doi.org/10.1021/ja00290a024
112. Ren X, Pickup PG (1994) Strong dependence of the electron-hopping rate in poly-tris(5-amino-1,10-phenanthroline)iron(III/II) on the nature of the counter-anion. J Electroanal Chem 365:289–292. https://doi.org/10.1016/0022-0728(93)03052-Q
113. Heinze J, Störzbach M, Mortensen J (1987) Experimental and theoretical studies on the redox properties of conducting polymers. Ber Bunsenges Phys Chem 91:960–967. https://doi.org/10.1002/bbpc.19870910926
114. Glarum SH, Marshall JH (1986) In situ potential dependence of poly(aniline) paramagnetism. J Phys Chem 90:6076–6077. https://doi.org/10.1021/j100281a005
115. Macdiarmid AG, Chiang J-C, Richter AF, Epstein AJ (1987) Polyaniline: a new concept in conducting polymers. Synth Met 18:285–290. https://doi.org/10.1016/0379-6779(87)90893-9
116. Kaya M, Kitani A, Sasaki K (1986) EPR studies of the charging process of polyaniline electrodes. Chem Lett 15:147–150. https://doi.org/10.1246/cl.1986.147
117. Genies EM, Lapkowski M (1987) Electrochemical in situ epr evidence of two polaron-bipolaron states in polyaniline. J Electroanal Chem Interfacial Electrochem 236:199–208. https://doi.org/10.1016/0022-0728(87)88027-0
118. Lapkowski M, Geniés EM (1990) Evidence of two kinds of spin in polyaniline from in situ EPR and electrochemistry: influence of the electrolyte composition. J Electroanal Chem Interfacial Electrochem 279:157–168. https://doi.org/10.1016/0022-0728(90)85173-3
119. MacDiarmid AG, Yang LS, Huang WS, Humphrey BD (1987) Polyaniline: electrochemistry and application to rechargeable batteries. Synth Met 18:393–398. https://doi.org/10.1016/0379-6779(87)90911-8
120. Genoud F, Guglielmi M, Nechtschein M et al (1985) ESR study of electrochemical doping in the conducting polymer polypyrrole. Phys Rev Lett 55:118–121
121. Genies EM, Pernaut JM (1984) Spectroelectrochemical studies of the redox and kinetic behaviour of polypyrrole film. Synth Met 10:117–129. https://doi.org/10.1016/0379-6779(84)90087-0

122. Kaufman JH, Colaneri N, Scott JC, Street GB (1984) Evolution of polaron states into bipolarons in polypyrrole. Phys Rev Lett 53: 1005–1008. https://doi.org/10.1103/PhysRevLett.53.1005
123. Genies EM, Lapkowski M (1987) Spectroelectrochemical study of polyaniline versus potential in the equilibrium state. J Electroanal Chem 220:67–82. https://doi.org/10.1016/0022-0728(87)88005-1
124. Neudeck A, Petr A, Dunsch L (1999) Redox mechanism of polyaniline studied by simultaneous ESR-UV-vis spectroelectrochemistry. Synth Met 107:143–158. https://doi.org/10.1016/S0379-6779(99)00135-6
125. Neudeck A, Petr A, Dunsch L (1999) Of the ultraviolet-visible spectra of the redox states of conducting polymers by simultaneous use of electron-spin resonance and ultraviolet-visible spectroscopy. J Phys Chem B 103:912–919
126. Paasch G, Nguyen PH, Fisher AJ (1998) Potential dependence of polaron and bipolaron densities in conducting polymers: theoretical description beyond the Nernst equations. Chem Phys 227:219–241. https://doi.org/10.1016/S0301-0104(97)00295-4
127. Epstein AJ, Ginder JM, Ritcher AF, MacDiarmid AG (1987) Conducting polymers. Alcácer L. D.Reidel, Dordrecht
128. Staftrom S, Bredas JL, Epstein AJ et al (1987) Polaron lattice in highly conducting polyaniline. Phys Rev Lett 59:1464. https://doi.org/10.1103/PhysRevLett.59.1464
129. Cavazzoni C, Colle R, Farchioni R, Grosso G (2004) Ab initio molecular dynamics study of the structure of emeraldine base polymers. Phys Rev B 69:115213. https://doi.org/10.1103/PhysRevB.69.115213
130. Varela-Alvarez A, J a S, Scuseria GE (2005) Doping of polyaniline by acid-base chemistry: density functional calculations with periodic boundary conditions. J Am Chem Soc 127: 11318–11327. https://doi.org/10.1021/ja051012t
131. Alemán C, Ferreira CA, Torras J et al (2008) On the molecular properties of polyaniline: a comprehensive theoretical study. Polymer (Guildf) 49:5169–5176. https://doi.org/10.1016/j.polymer.2008.09.023
132. Canales M, Torras J, Fabregat G et al (2014) Polyaniline Emeraldine salt in the amorphous solid state: polaron versus bipolaron. J Phys Chem B 118:11552–11562. https://doi.org/10.1021/jp5067583
133. Cavazzoni C, Colle R, Farchioni R, Grosso G (2006) HCl-doped conducting Emeraldine polymer studied by ab initio car-parrinello molecular dynamics. Phys Rev B 74:33103. https://doi.org/10.1103/PhysRevB.74.033103
134. Bernard MC, Hugot-Le Goff A (2006) Quantitative characterization of polyaniline films using Raman spectroscopy. Electrochim Acta 52:595–603. https://doi.org/10.1016/j.electacta.2006.05.039
135. Epstein AJ, Macdiarmid AG (1988) Protonation of emeraldine: formation of a granular polaronic polymeric metal. Mol Cryst Liq Cryst Inc Nonlinear Opt 160:165–173. https://doi.org/10.1080/15421408808083011
136. Cushman RJ, McManus PM, Cheng Yang S (1987) Spectroelectrochemical study of polyaniline: the construction of a pH-potential phase diagram. J Electroanal Chem 219:335–346. https://doi.org/10.1016/0022-0728(87)85051-9
137. Stilwell D, Park SM (1988) Electrochemistry of conductive polymers V. in situ spectroelectrochemical studies of polyaniline films. J Electrochem Soc 136:427–433. https://doi.org/10.1149/1.2220844
138. Chinn D, DuBow J, Li J et al (1995) Comparison of chemically and electrochemically prepared polyaniline films. 2. Optical properties. Chem Mater 7:1510–1518. https://doi.org/10.1021/cm00056a017
139. Nekrasov AA, Ivanov VF, Vannikov AV (2000) Analysis of the structure of polyaniline absorption spectra based on spectroelectrochemical data. J Electroanal Chem 482:11–17. https://doi.org/10.1016/S0022-0728(00)00005-X
140. Nekrasov AA, Ivanov VF, Vannikov AV (2001) Effect of pH on the structure of absorption spectra of highly protonated polyaniline analyzed by the Alentsev-Fock method. Electrochim Acta 46: 4051–4056. https://doi.org/10.1016/S0013-4686(01)00693-4
141. Kankare J, Kupila E-L (1992) In-situ conductance measurement during electropolymerization. J Electroanal Chem 322:167–181. https://doi.org/10.1016/0022-0728(92)80074-E
142. Chiang J-C, MacDiarmid AG (1986) 'Polyaniline': protonic acid doping of the emeraldine form to the metallic regime. Synth Met 13:193–205. https://doi.org/10.1016/0379-6779(86)90070-6
143. Epstein AJ, Ginder JM, Zuo F et al (1987) Insulator-to-metal transition in polyaniline: effect of protonation in emeraldine. Synth Met 21:63–70. https://doi.org/10.1016/0379-6779(87)90067-1
144. Luthra V, Singh R, Gupta SK, Mansingh A (2003) Mechanism of dc conduction in polyaniline doped with sulfuric acid. Curr Appl Phys 3:219–222. doi: https://doi.org/10.1016/S1567-1739(02)00205–5
145. McManus PM, Cushman RJ, Yang SC (1987) Influence of oxidation and protonation on the electrical conductivity of polyaniline. J Phys Chem 91:744–747. https://doi.org/10.1021/j100287a050
146. Paul EW, Ricco AJ, Wrighton MS (1985) Resistance of polyaniline films as a function of electrochemical potential and the fabrication of polyaniline-based microelectronic devices. J Phys Chem 89:1441–1447. https://doi.org/10.1021/j100254a028
147. Ofer D, Crooks RM, Wrighton MS (1990) Potential dependence of the conductivity of highly oxidized poly thiophenes, polypyrroles, and poly aniline: finite windows of high conductivity. J Am Chem Soc 112:7869–7879. https://doi.org/10.1021/ja00178a004
148. Talaie A (1994) Electronic Propenies of novel conducting polypyrrole and polyaniline materials. Wollongong University
149. Song E, Choi J-W (2012) An on-chip chemiresistive polyaniline nanowire-based pH sensor with self-calibration capability. 2012 Annu. Int. Conf. IEEE Eng. Med. Biol. Soc.
150. Chen F, He J, Nuckolls C et al (2005) A molecular switch based on potential-induced changes of oxidation state. Nano Lett 5:503–506. https://doi.org/10.1021/nl0478474
151. Toušek J, Toušková J, Chomutová R et al (2017) Mobility of holes and polarons in polyaniline films assessed by frequency-dependent impedance and charge extraction by linearly increasing voltage. Synth Met 234:161–165. https://doi.org/10.1016/j.synthmet.2017.10.015
152. Babu VJ, Vempati S, Ramakrishna S (2013) Conducting polyaniline-electrical charge transportation. Mater Sci Appl 04: 1–10. https://doi.org/10.4236/msa.2013.41001
153. Stejskal J, Bogomolova OE, Blinova NV et al (2009) Mixed electron and proton conductivity of polyaniline films in aqueous solutions of acids: beyond the 1000 S cm-1 limit. Polym Int 58:872–879. https://doi.org/10.1002/pi.2605
154. Hu C-C, Chu C-H (2001) Electrochemical impedance characterization of polyaniline-coated graphite electrodes for electrochemical capacitors — effects of film coverage/thickness and anions. J Electroanal Chem 503:105–116. https://doi.org/10.1016/S0022-0728(01)00385-0
155. Lizarraga L, Andrade EM, Molina FV (2004) Swelling and volume changes of polyaniline upon redox switching. J Electroanal Chem 561:127–135. https://doi.org/10.1016/j.jelechem.2003.07.026

156. Lizarraga L, Andrade EM, Molina FV (2007) Anion exchange influence on the electrochemomechanical properties of polyaniline. Electrochim Acta 53:538–548. https://doi.org/10.1016/j.electacta.2007.07.030

157. Inzelt G (2000) Simultaneous chronoamperometric and quartz crystal microbalance studies of redox transformations of polyaniline films. Electrochim Acta 45:3865–3876. https://doi.org/10.1016/S0013-4686(00)00455-2

158. Inzelt G (1995) Characterization of modified electrodes by electrochemical quartz crystal microbalance, radiotracer technique and impedance spectroscopy. Electroanalysis 7:895–903. https://doi.org/10.1002/elan.1140070918

159. Pruneanu S, Csahók E, Kertész V, Inzelt G (1998) Electrochemical quartz crystal microbalance study of the influence of the solution composition on the behaviour of poly(aniline) electrodes. Electrochim Acta 43:2305–2323. https://doi.org/10.1016/S0013-4686(97)10154-2